Tecniche di imaging in medicina: sviluppi tecnologici e loro applicazioni

Tecniche di imaging in medicina: sviluppi tecnologici e loro applicazioni

N. Belcari, M.G. Bisogni, L. Biagi, N. Camarlinghi, M. Cecchetti , M. Costagli, A. Del Guerra, P. Delogu, M.E. Fantacci, S. Ferretti, A. Kraan, B. Liu, N. Marino, M. Morrocchi, A. Retico, D. Scelfo, R. Stara, V. Rosso, G. Sportelli, A. Stefanini, K. Straub, G. Tiberi, A. Toncelli, M. Tosetti

PROGRAMMI DI RICERCA SCIENTIFICA DI RILEVANTE INTERESSE NAZIONALE
Anno 2010-2011 - prot. 2010P98A75

INSIDE: INnovative Solutions for In-beam DosimEtry in Hadrontherapy

1	Università di PISA	A. Del Guerra
2	Politecnico di BARI	F. Corsi
3	INFN	G. Battistoni
4	Univ. di ROMA "La Sapienza"	V. Patera
5	Università di TORINO	C. Peroni

PROGRAMMI DI RICERCA SCIENTIFICA DI RILEVANTE INTERESSE NAZIONALE
Anno 2010-2011 - prot. 2010P98A75

INSIDE aims to build a dedicated in-beam PET scanner, capable of:

- handling the count rate during the treatment
- reconstruct the Bragg peak position to 1 mm

» in less than 5 minutes since the beginning of dose delivery.

Keywords:
HADRON THERAPY
IN-BEAM PET
SILICON PHOTOMULTIPLIER (SiPM)

Hadron therapy

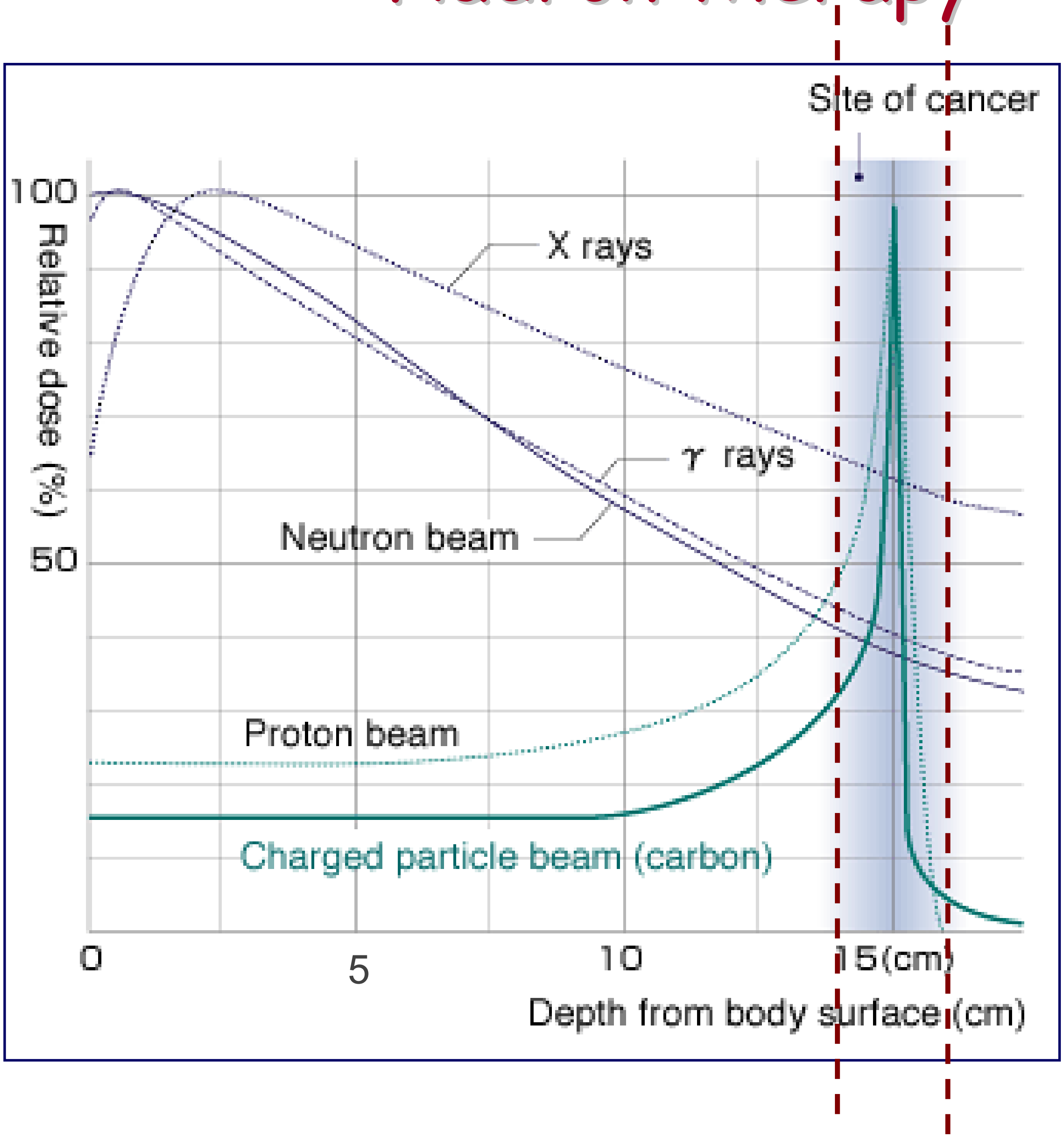

- ❑ Relatively low entrance dose (plateau)
- ❑ Maximum dose at depth (Bragg peak)
- ❑ Rapid distal dose fall-off
- ❑ Energy modulation (Spread-out Bragg peak)
- ❑ Enhanced RBE

Hadron therapy

Relative biological effectiveness

$$RBE = \frac{D_{RX}}{D_r}$$

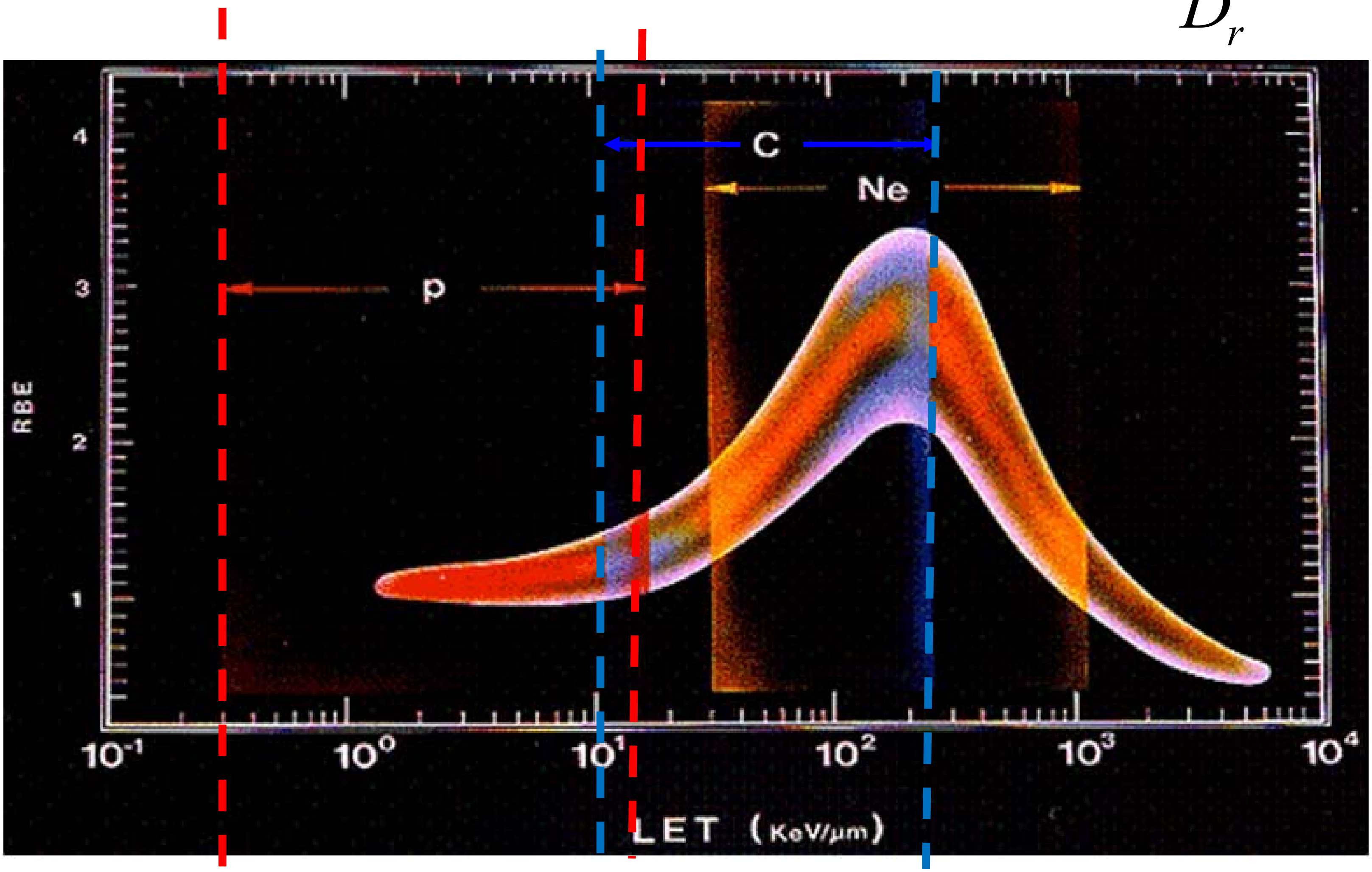

$$E = D * RBE * w$$

Hadron therapy

Physical advantages of hadron beams

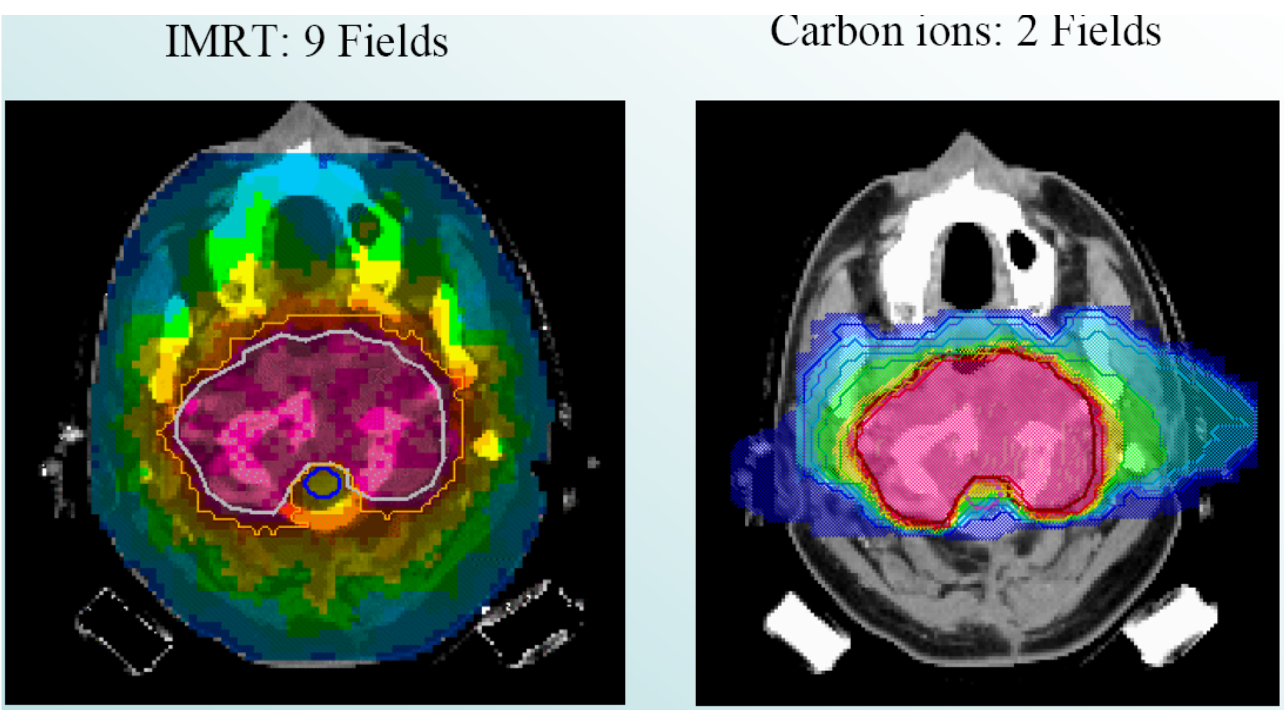

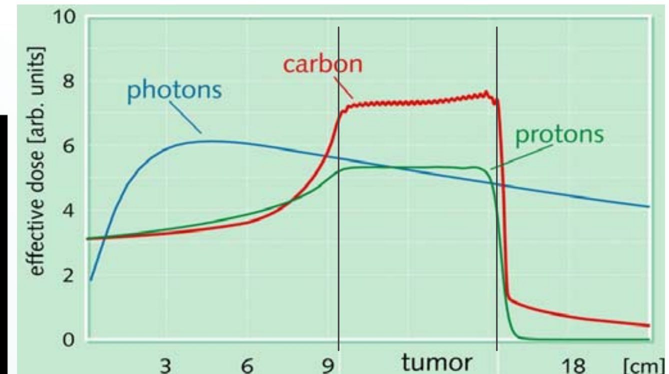

exponential attenuation
vs
Bragg peak

- Increase of conformity and reduction of integral dose;
- Improve local control rate;
- Higher survival rate.

M Kraemer and M Scholz, 2000, Treatment planning for heavy ion therapy Phys. Med. Biol. 45 3319–30

Hadron therapy

Nuclear fragmentation

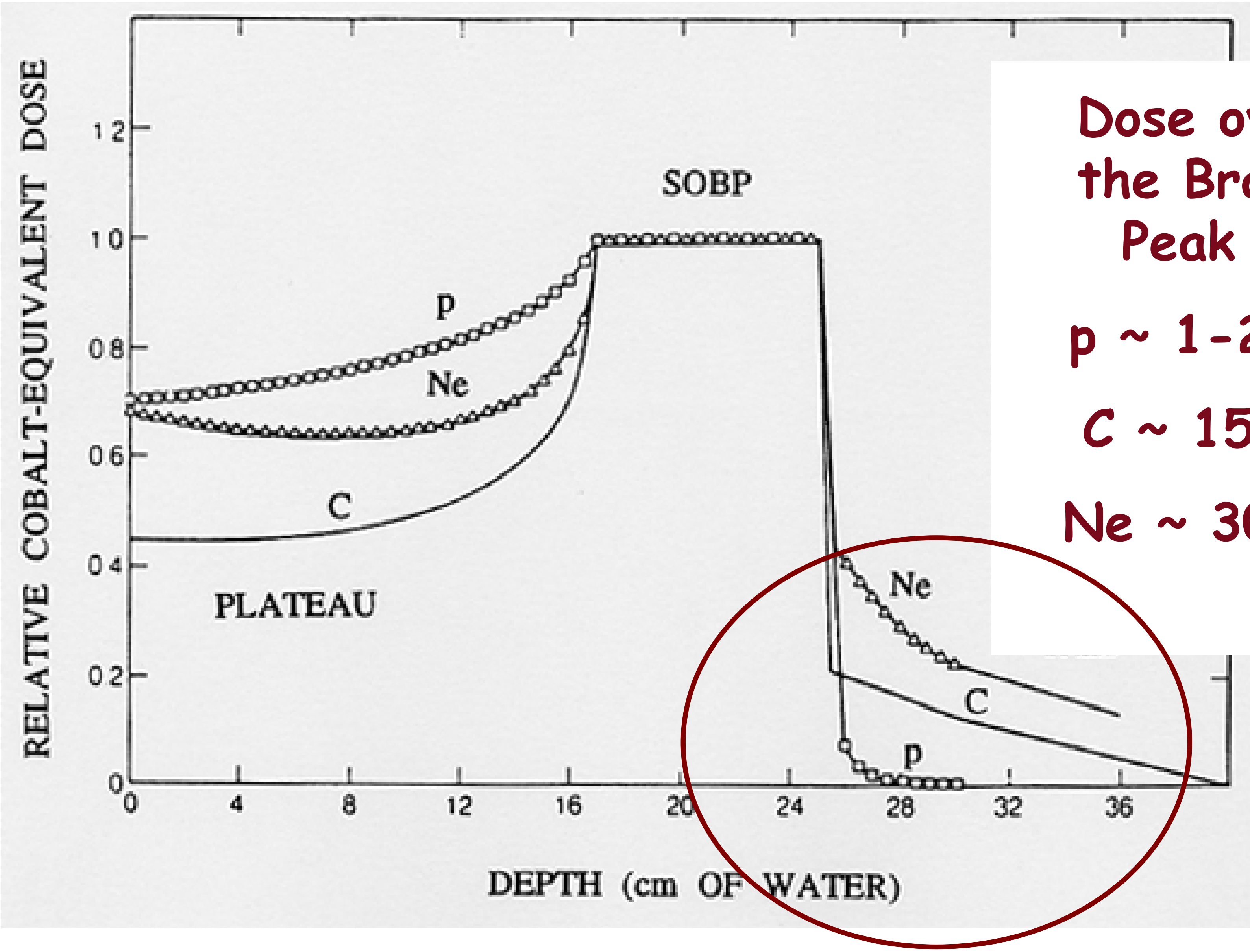

Dose over the Bragg Peak :

p ~ 1-2 %

C ~ 15 %

Ne ~ 30 %

Hadron therapy

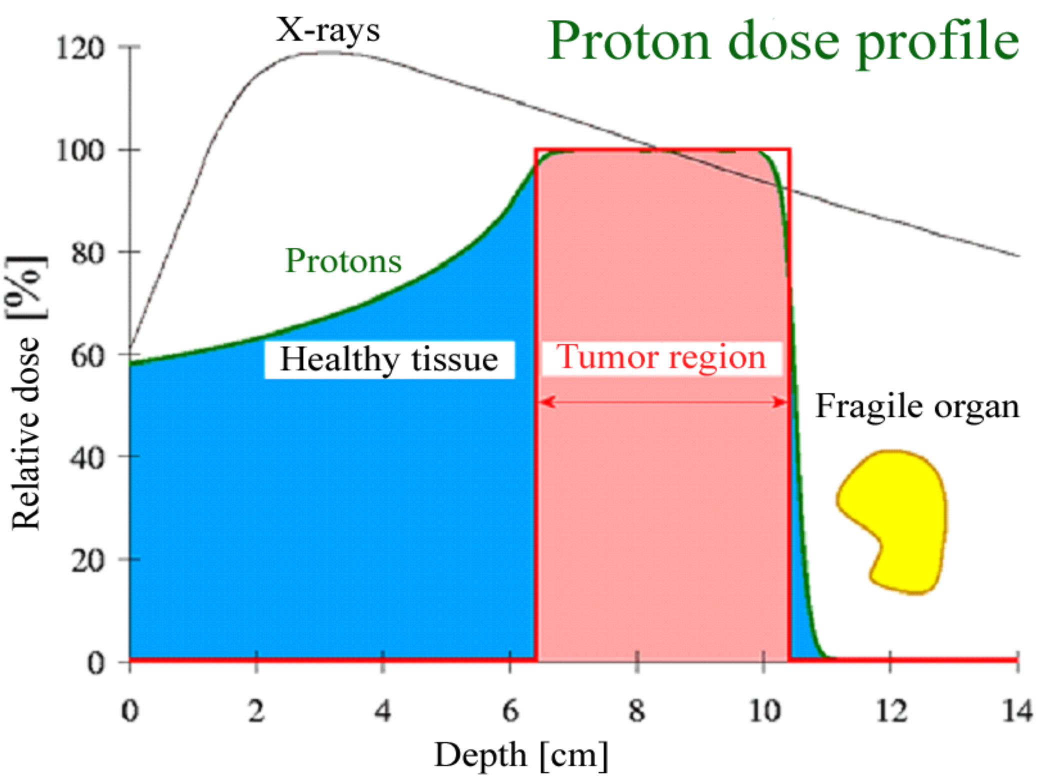

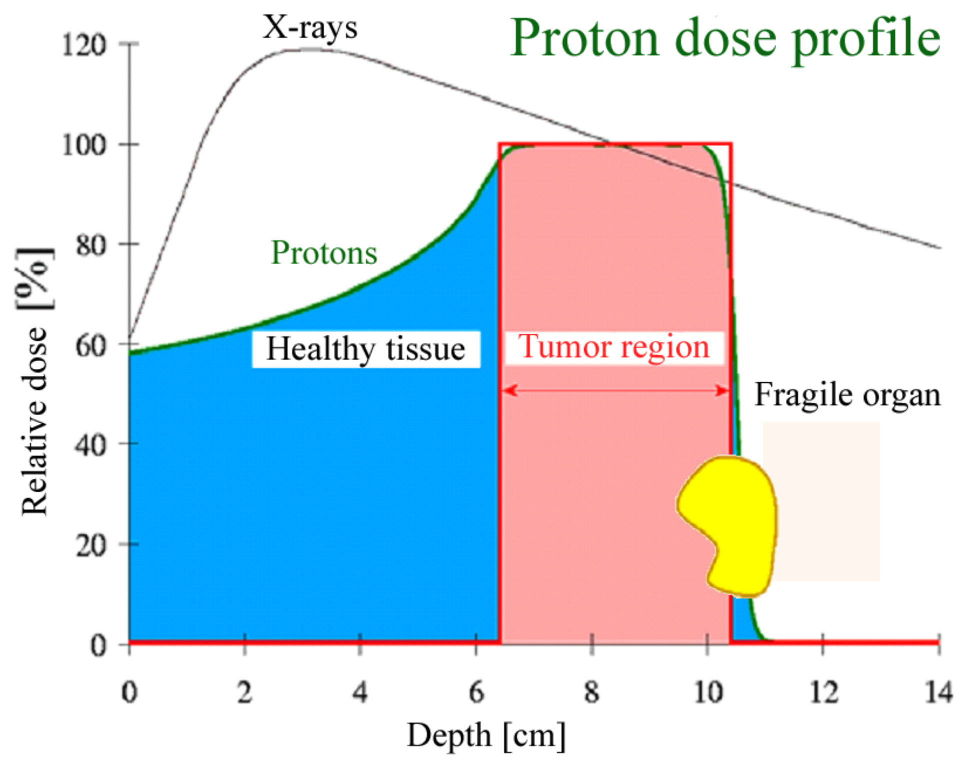

If we miss the target (for whatever reason) we can cause a damage

This is a new challenge- it's not much of a problem for X-rays

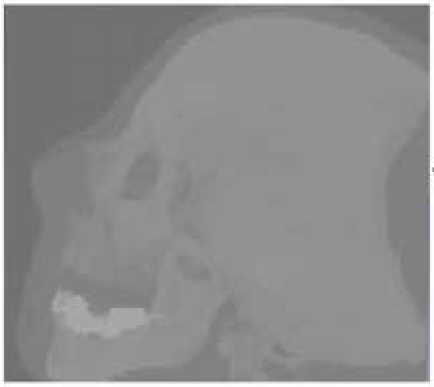

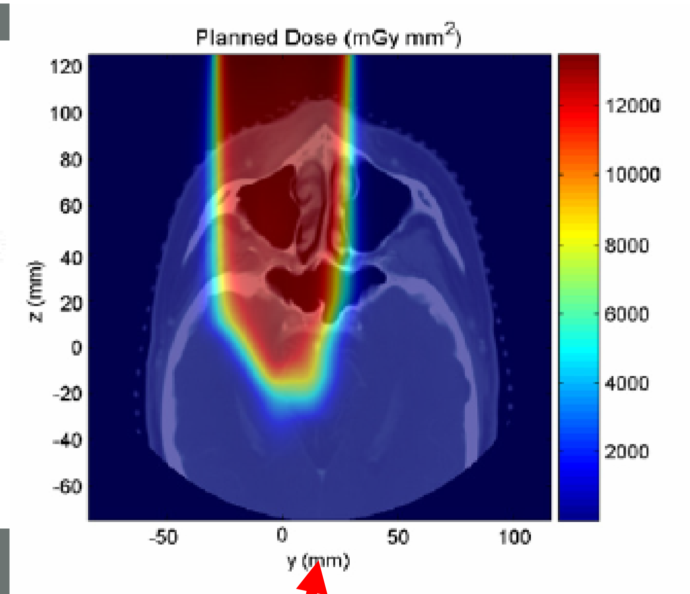

urance:

dose

lative biological

logy related

fectiveness

BE)

NTIES

chine related

vice tolerances

am energy

The Treatment Planning System (TPS)

Input
3D Information (CT,MRI,PET) $\rightarrow$ **TPS** $\rightarrow$ **Output** $\{\phi_i, E_{Ki}, \theta_i\}$

$i \rightarrow$ i-th beam

$\phi_i \rightarrow$ fluence

$E_{Ki} \rightarrow$ kinetic energy

$\theta_i \rightarrow$ direction

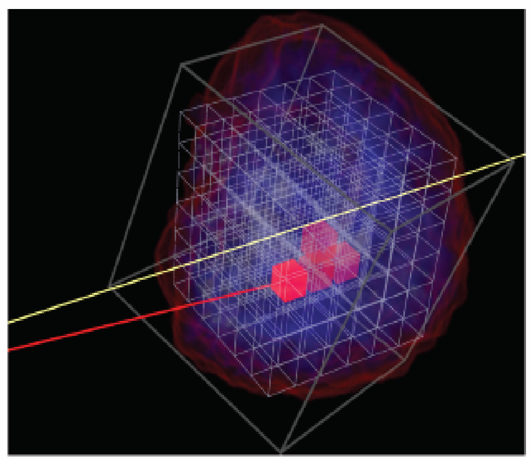

Hadron therapy

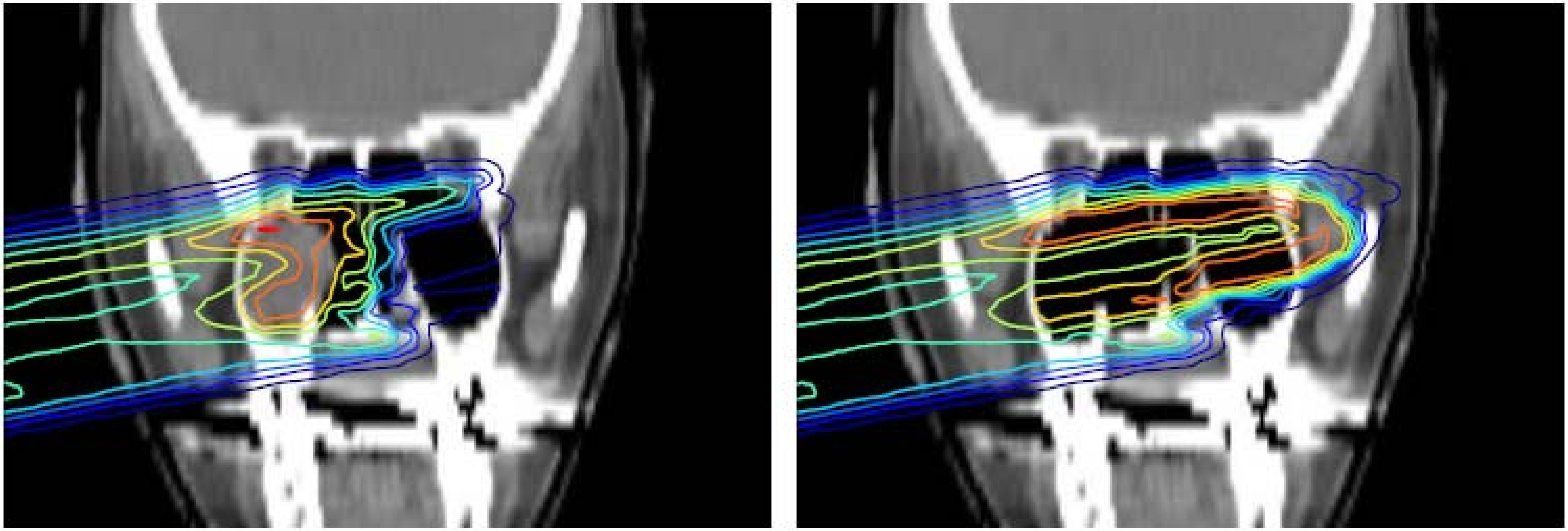

Planned

.. but a tissues reduction followed

Necessity of monitoring!

K. Parodi et al., IJROBP 68 (2007)

Hadron therapy

In this context, among different possibilities, Positron Emission Tomography (PET) is potentially a tool for in vivo, non invasive monitoring of the precision of the treatment in hadrontherapy.

- ❖ Gamma prompt
- ❖ Interaction vertex imaging (IVI)
- ❖ Proton CT

PRIN, V. Patera

The principle of PET monitoring

Therapeutic hadron beams produce in the biological tissues short - lived β^+ emitters by means of projectile and/or target nuclei fragmentations.

Protons:

$p + {}^{16}O$, (p,n) + ^{15}O

$T_{15\text{-}O}$=121.8 s

$p + {}^{12}C$, (p,n) + ^{11}C

$\tau_{11\text{-}C}$ =1222.8 s

Carbon:

^{12}C + p, ^{11}C + (p,n)

^{12}C + p, ^{10}C + (p,2n)

$\tau_{10\text{-}C}$ =19.3 s

The principle of PET monitoring

Therapeutic hadron beams produce in the biological tissues short - lived β^+ emitters by means of projectile and/or target nuclei fragmentations.

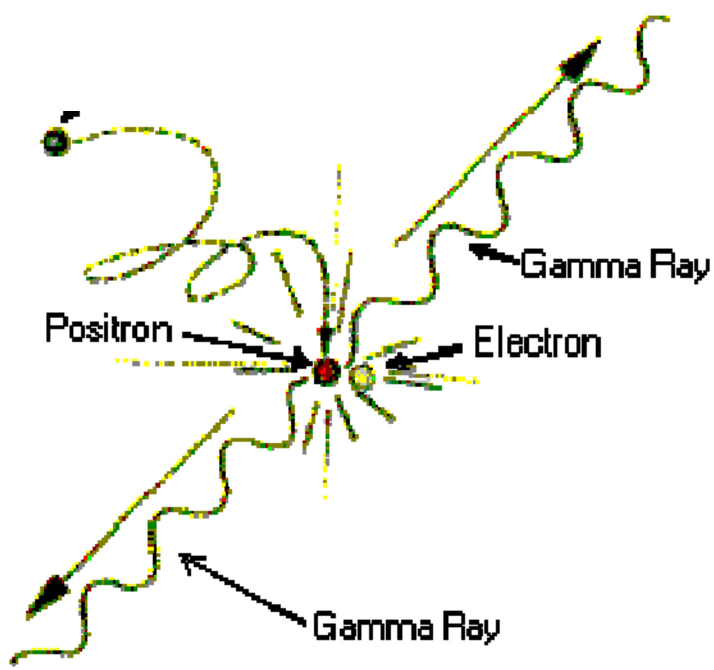

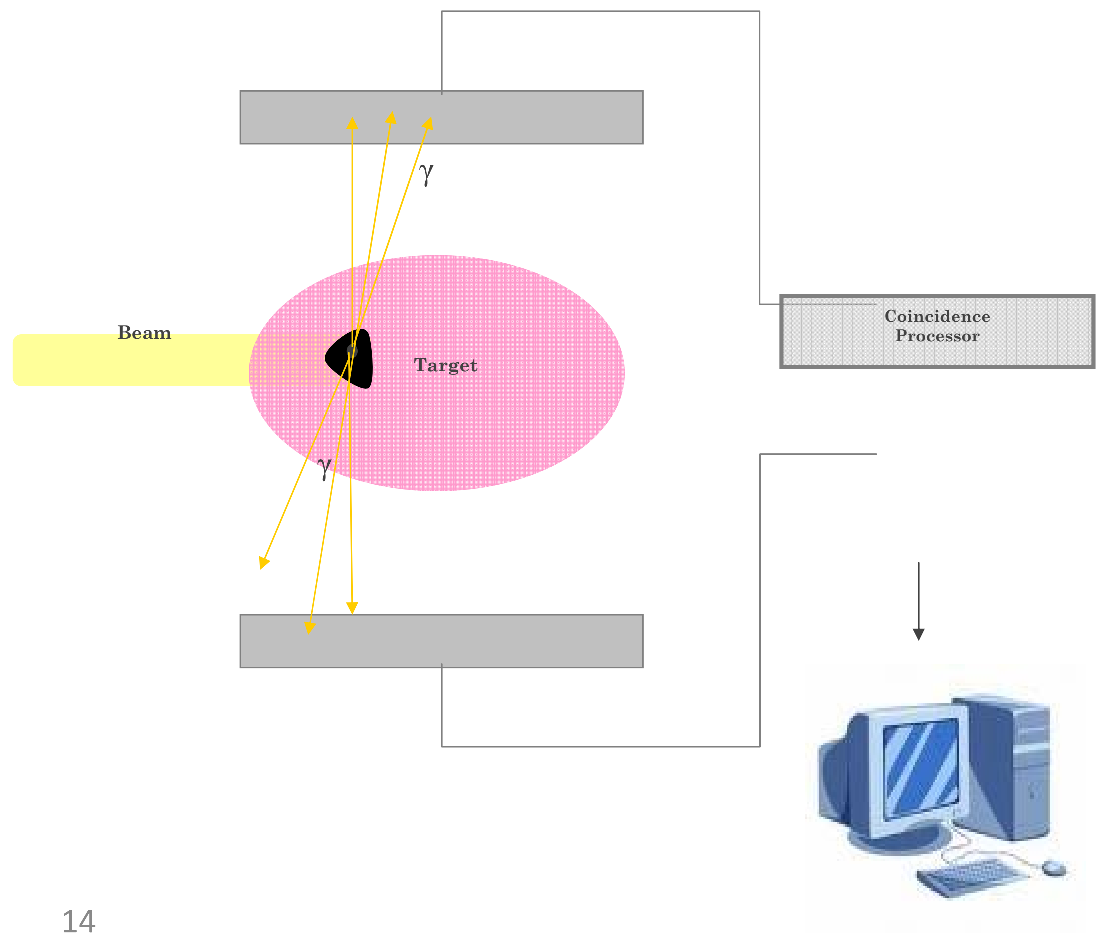

The principle of PET monitoring

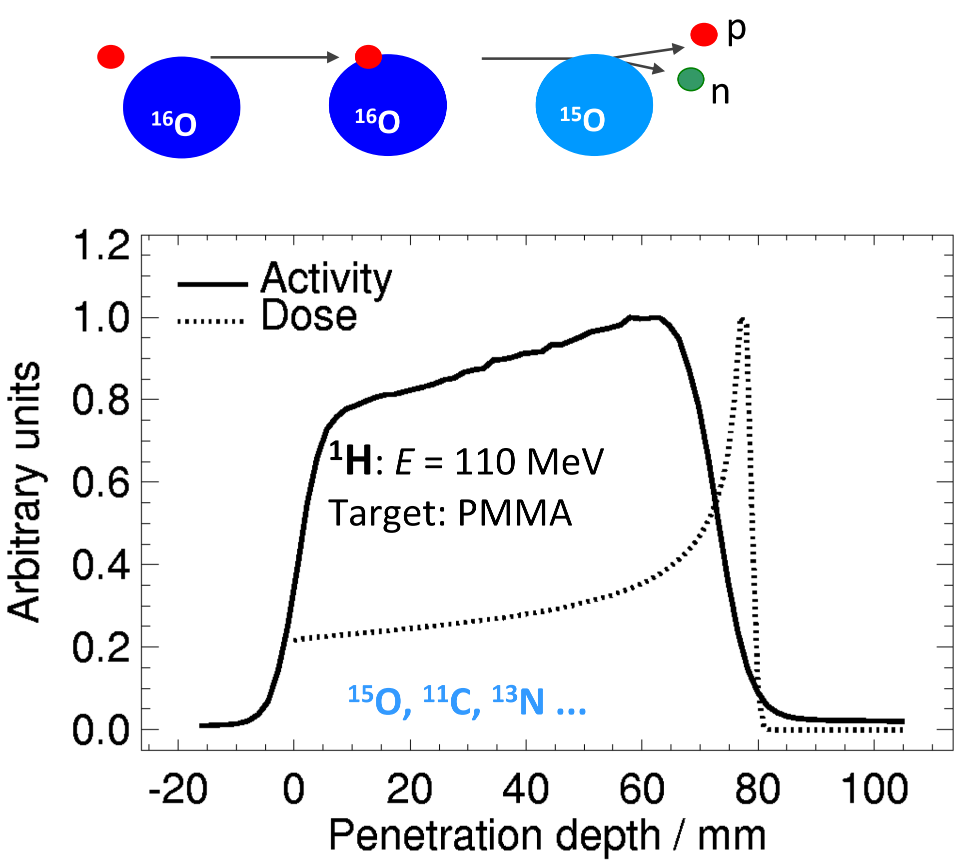

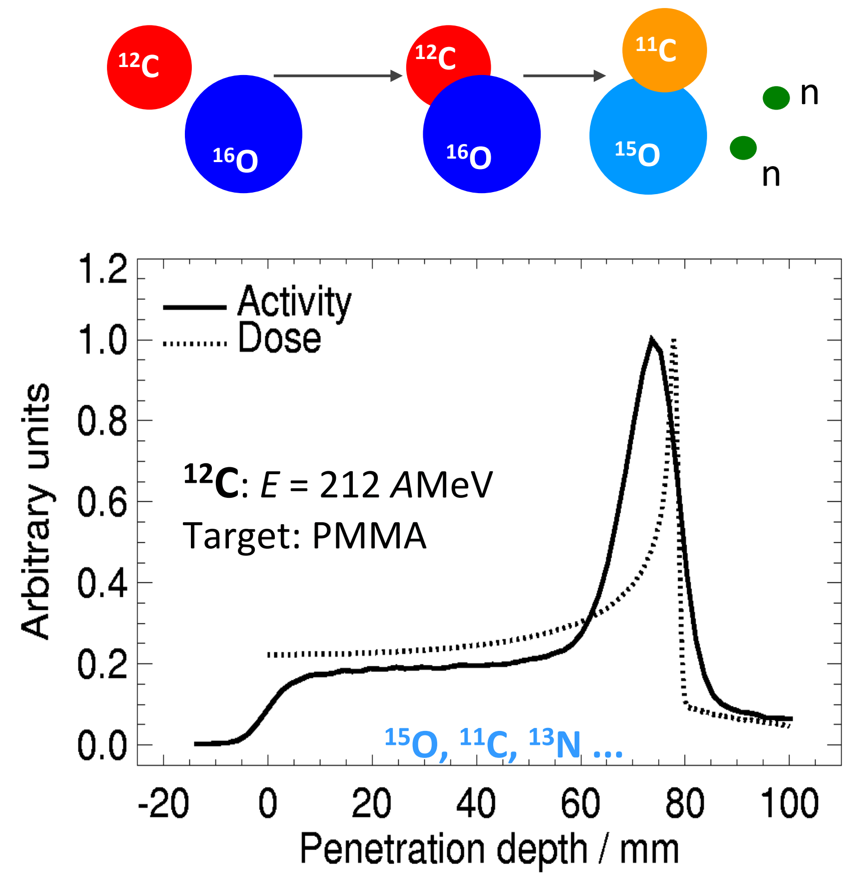

- Nuclear cross sections fall off at low energy just few millimeters before Bragg peak: 15-20 MeV threshold for p-induced nuclear reactions
- Finding the distribution of positron annihilation points it would be possible to extract non invasively in vivo information about dose localization.

J Pawelke et al., Proceeding: Ion Beams in Biology and Medicine (IBIBAM), 26.-29.09.2007, Heidelberg, Germany

DoPET: an in-beam PET monitor for hadrontherapy

N. Belcari, N. Camarlinghi, A. Del Guerra, S. Ferretti, A. Kraan, V. Rosso, G. Sportelli, K. Straub

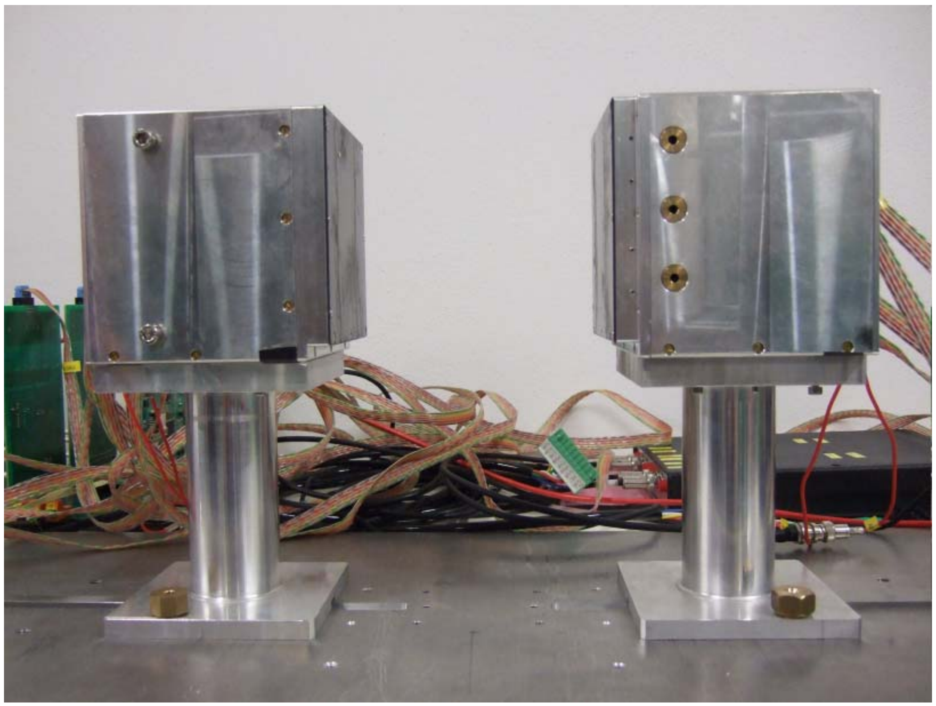

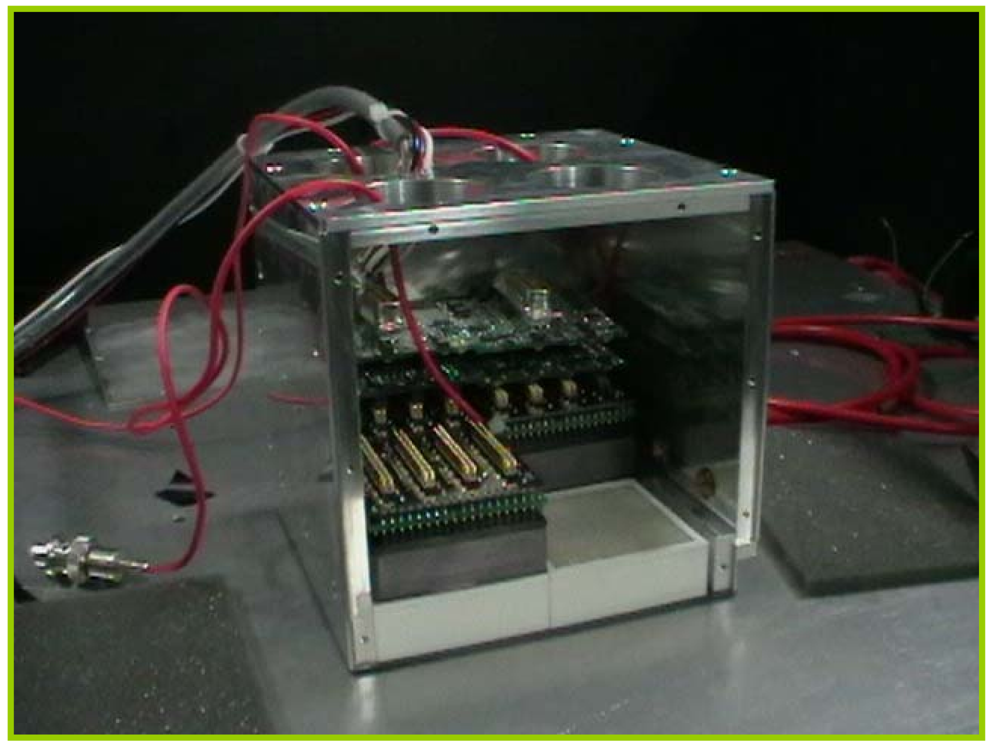

INFN Istituto Nazionale di Fisica Nucleare

UNIVERSITÀ DI PISA

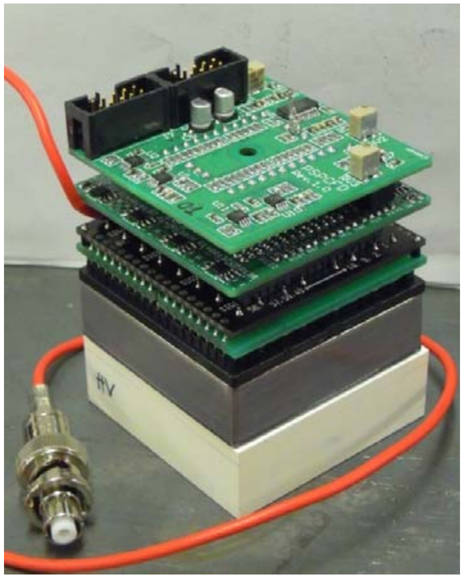

The Tomograph Architecture

Detector module

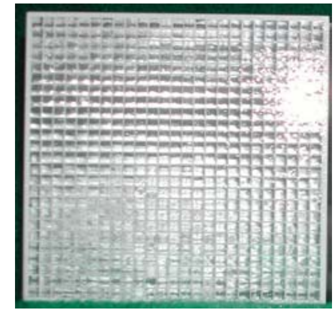

- Scintillating crystals LYSO:Ce from Hilger

  Crystals Ltd:
  - 23 x 23 pixels;
  - 2 x 2 x 16 mm^3 pixel dimensions.

- PS-PMT H8500 from Hamamatsu Photonics K.K.:
  - 49 x 49 mm^2 active area, 8 x 8 anodes;
  - 12 stage dynode.

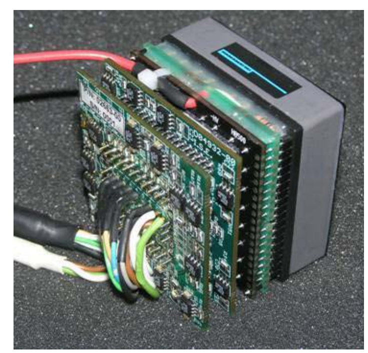

- Front-end electronics:
  - Resistive chain 64 inputs/8+8 outputs SCD

    (symmetric charge division);
  - 2D chain 8+8 inputs/2+2 outputs;
  - pre-amp (PSP).

Reconstruction and data analysis

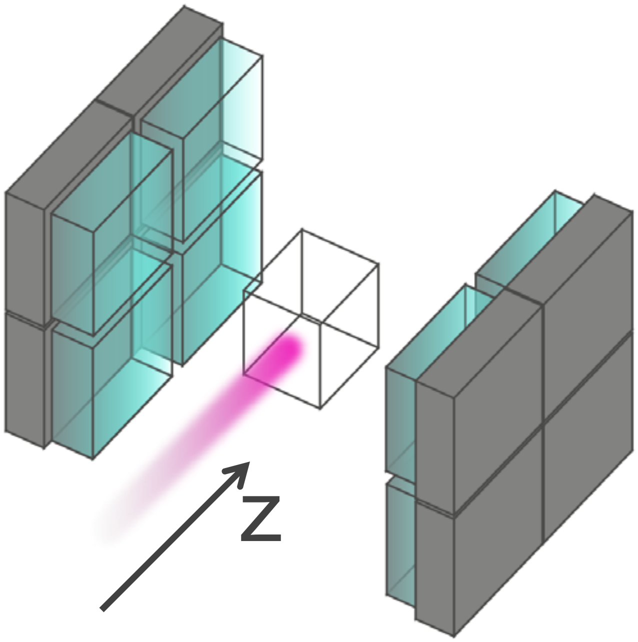

Image Reconstruction

System is underdetermined → Iterative Algorithm

Low statistics: → 3D Algorithm

The Adopted Solution: ML-EM

Maximum Likelihood -Expectation Maximization

Whithin the FoV we reconstruct:

- The 3D activity distribution
- the activity profile along z
- reference points @ 50% on proximal and distal activity distribution

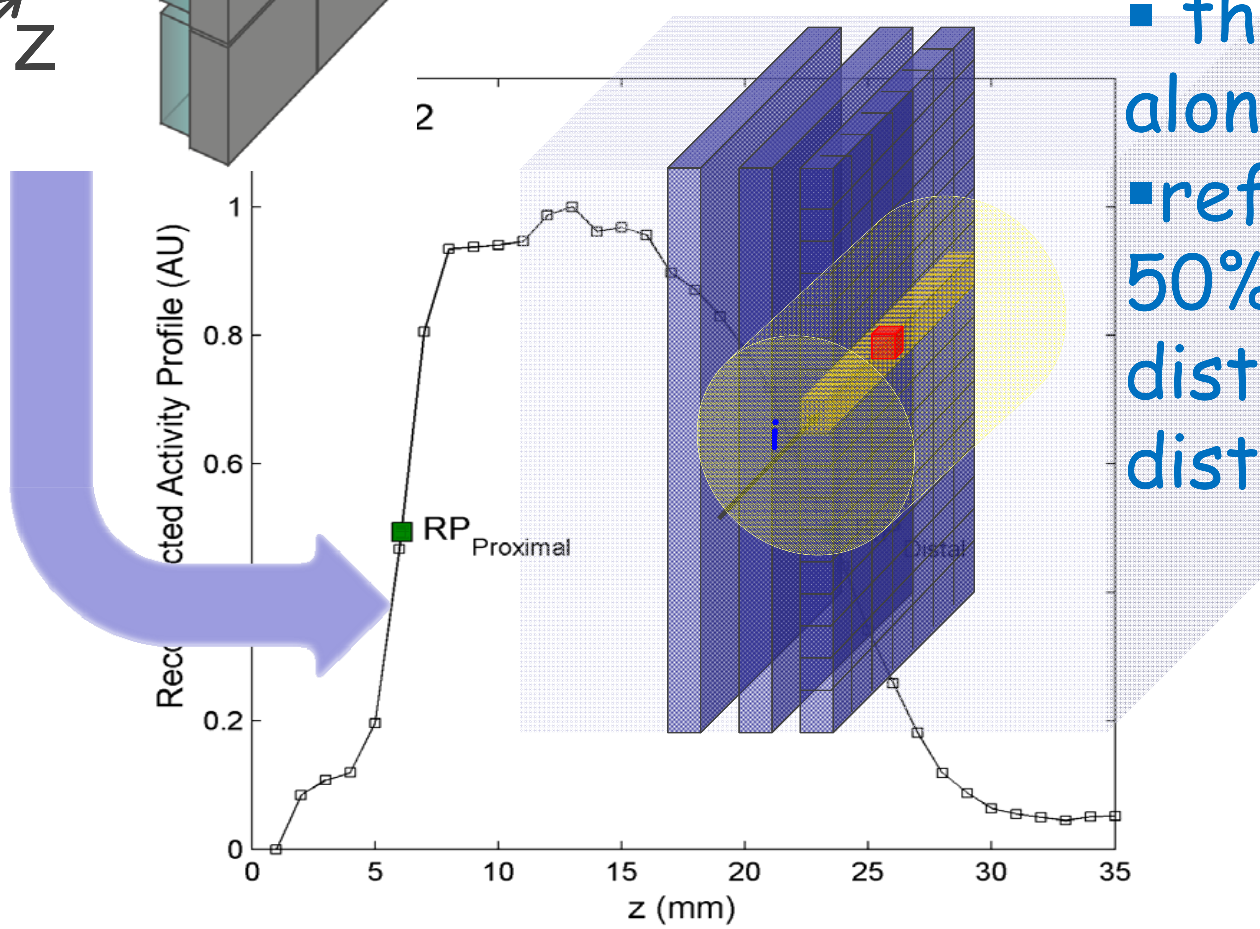

CATANA and CNAO experimental setups

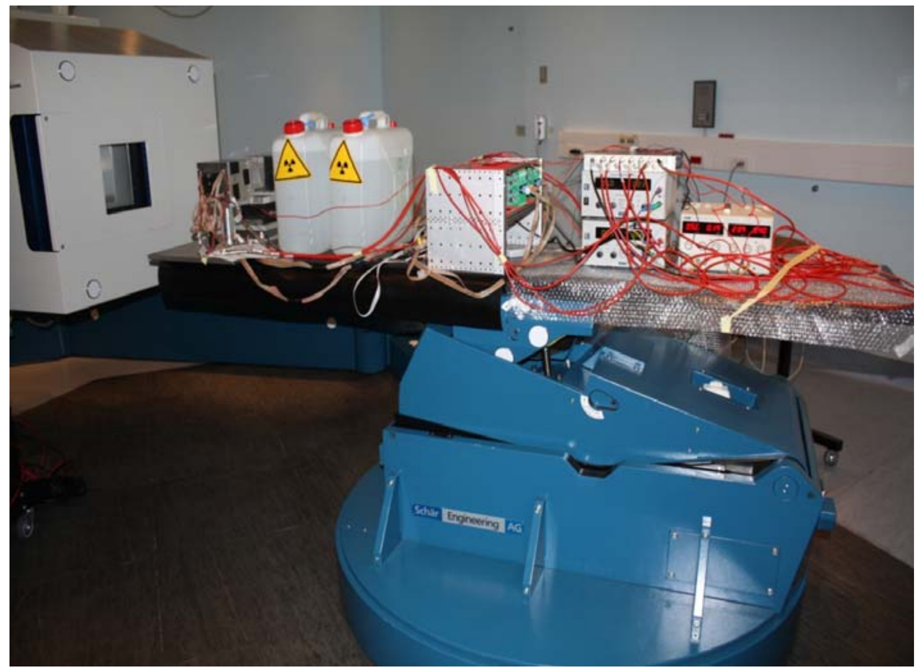

CNAO experimental setup

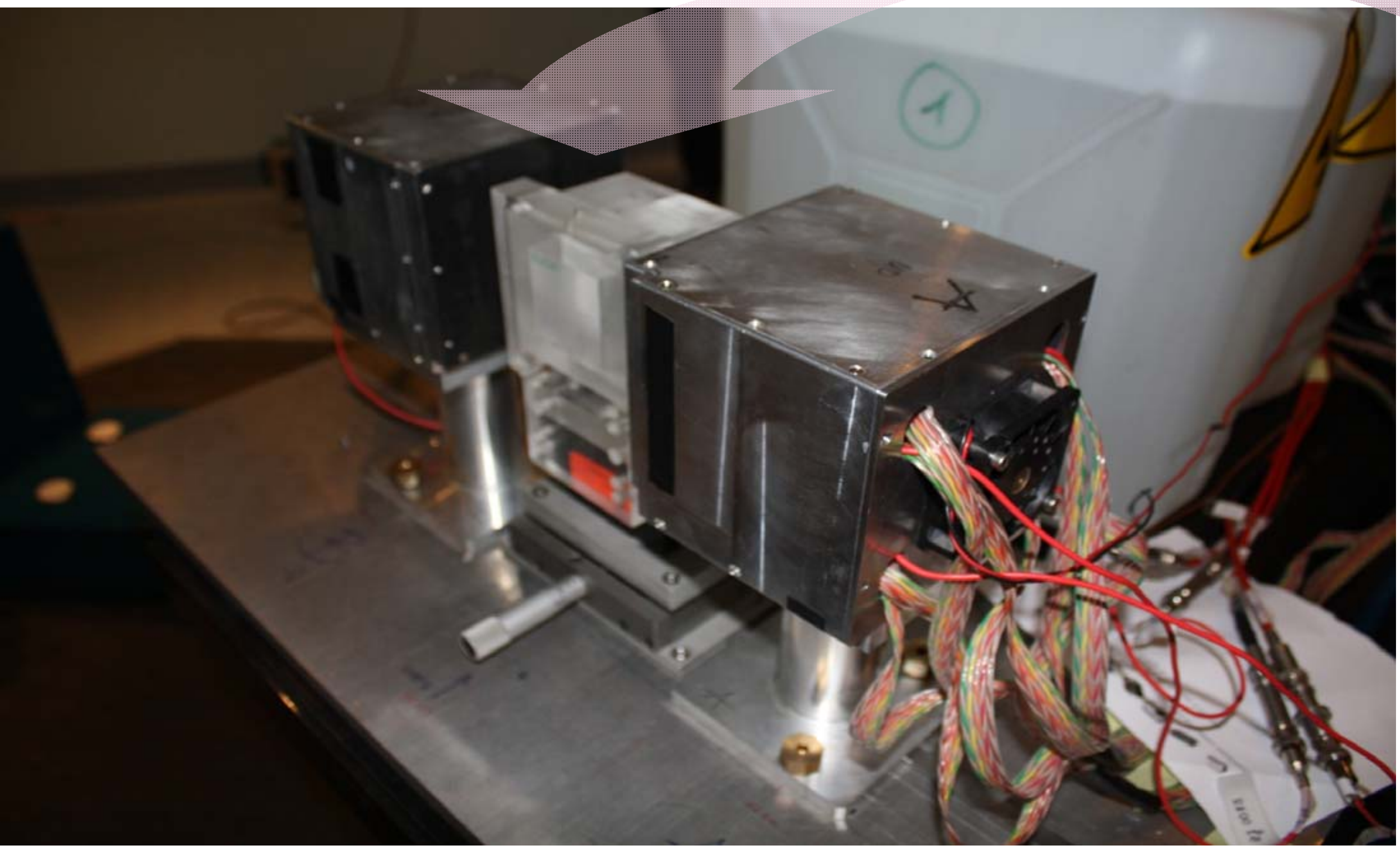

A PMMA phantom was irradiated with proton energies: 93, 97.5, 99, and 112 MeV

	Density	H(%)	C (%)	0 (%)	N (%)	Ca (%)
bone	1.819	3.41	31.41	36.50	1.64	26.81
PMMA	1.18	8	60	32		
muscle	1.050	8.10	67.12	19.85	2.42	2.31
brain	1.049	10.83	72.54	14.86	1.69	

CNAO data analysis

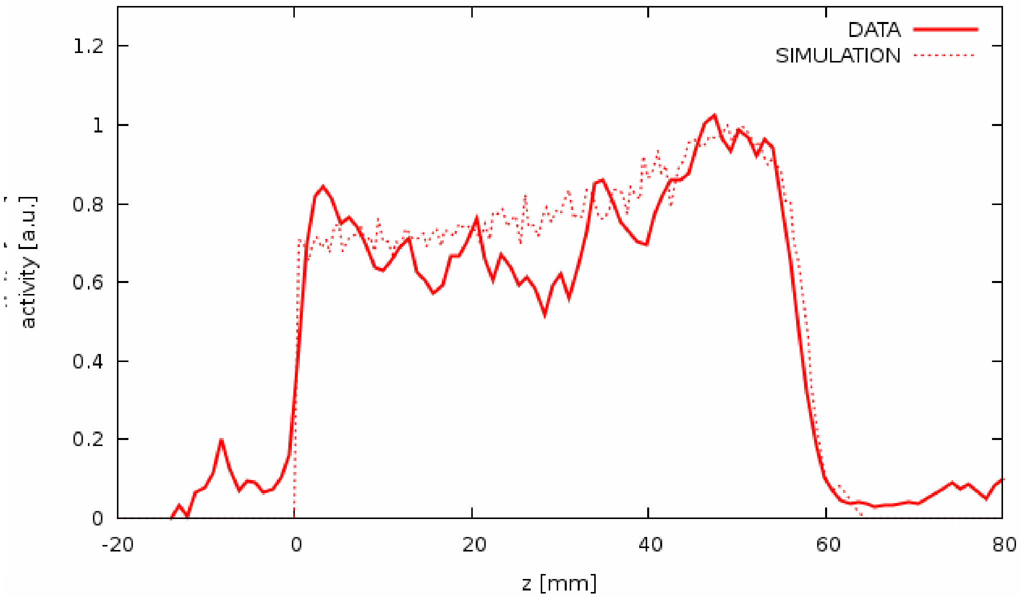

Comparison of the position of the 50% fall-off between FLUKA simulation and data for 99 MeV protons.

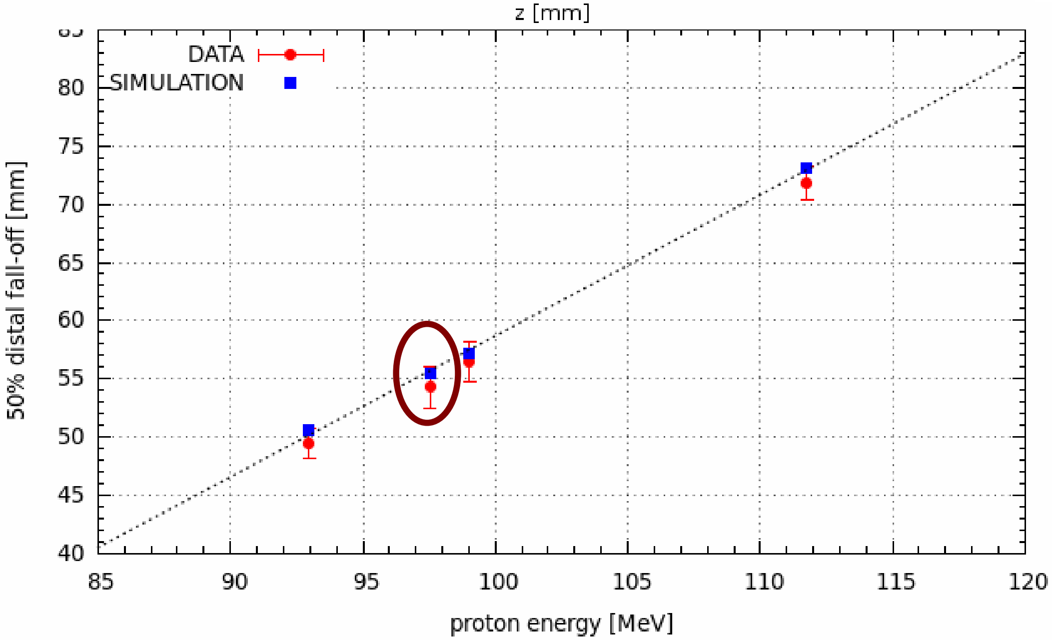

We evaluate a 1mm accuracy for the determination of the distal fall-off.

G. Battistoni, P. Sala, A. Ferrari, A. Mairani

Monitoring modalities

In-beam

- In-spill
- Intra-spill

Off-beam

- In-room
- Off-room

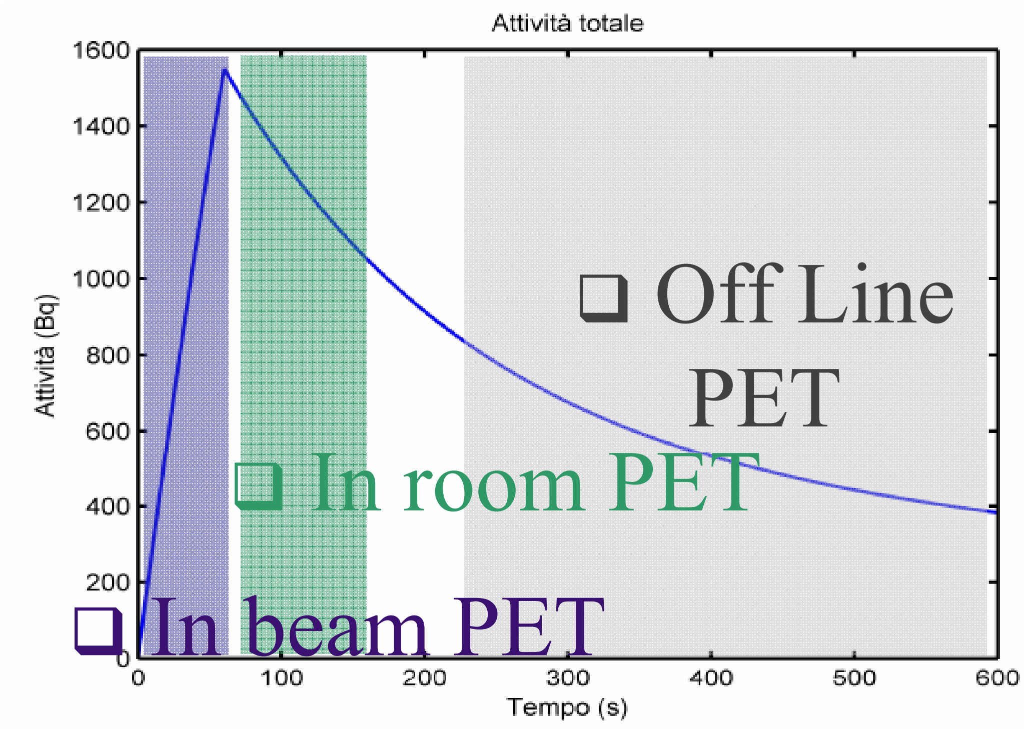

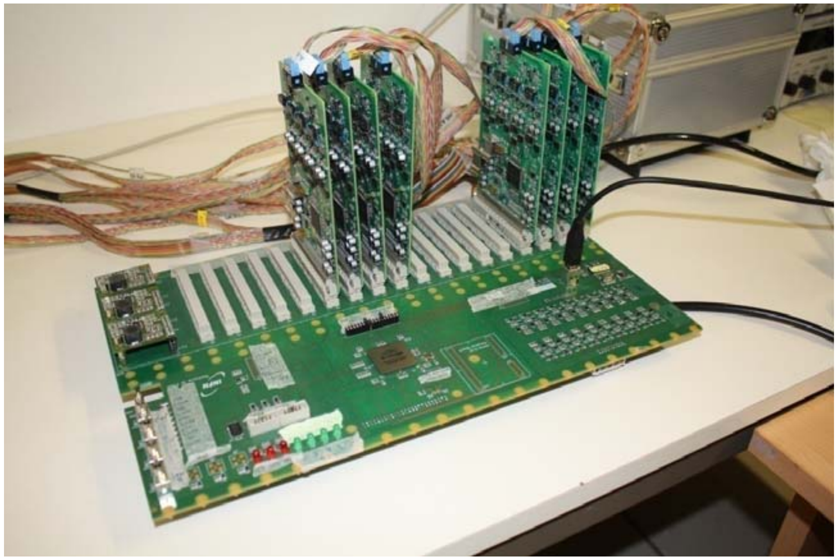

CNAO: in-beam and in-room monitoring

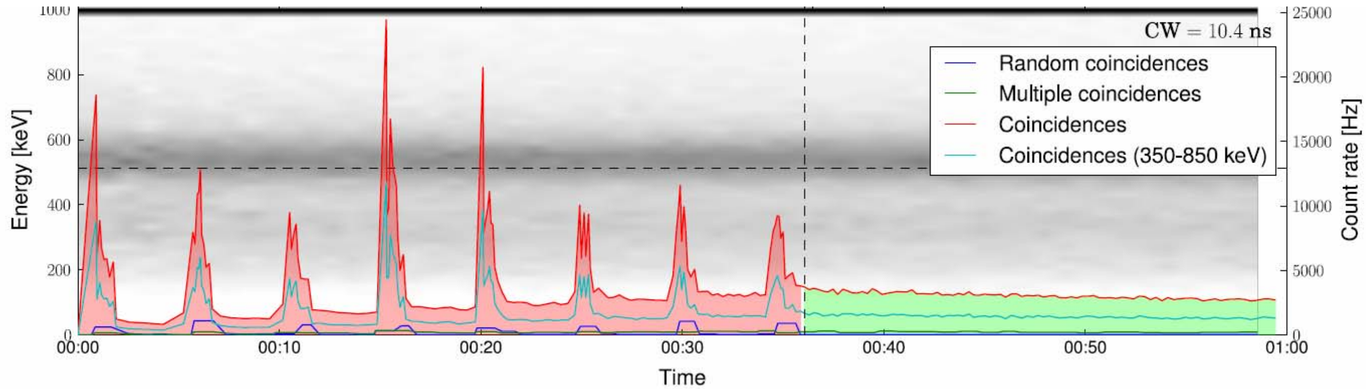

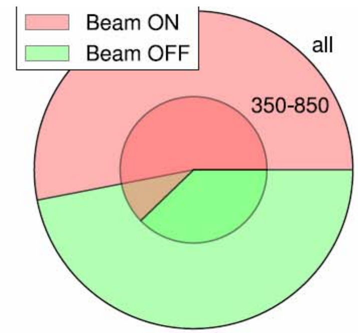

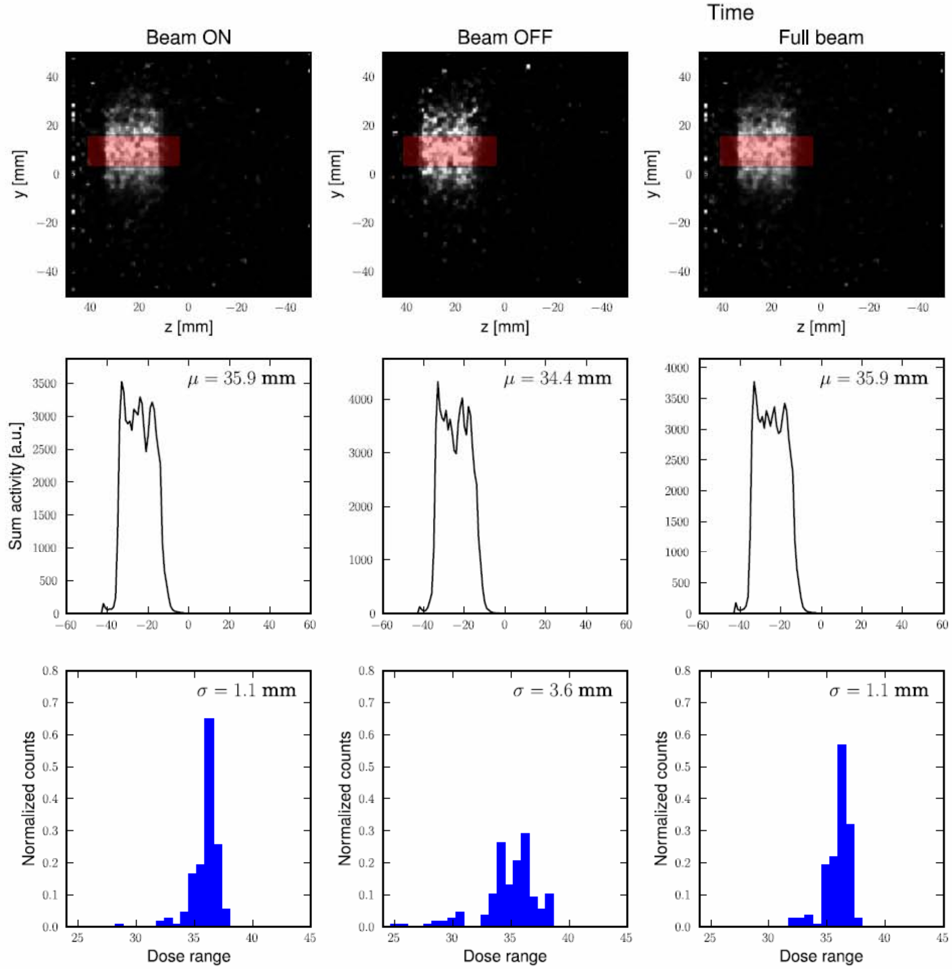

Facility: CNAO
Energy: 62.3 MeV
Dose at the peak: 20 Gy in 36 s (8 spills)
Acquisition time: 1 min

- Beam-ON data: 53%
- Beam-OFF data: 47%
- Data in the 350-850 EW: 46 %
- Beam-ON data in the EW: 62%
- Beam-OFF data in the EW: 38%

The standard deviation of particle ranges is about 1 mm for the beam-on PET image. Beam-off data is much less precise and does not contribute significantly to the measurement.

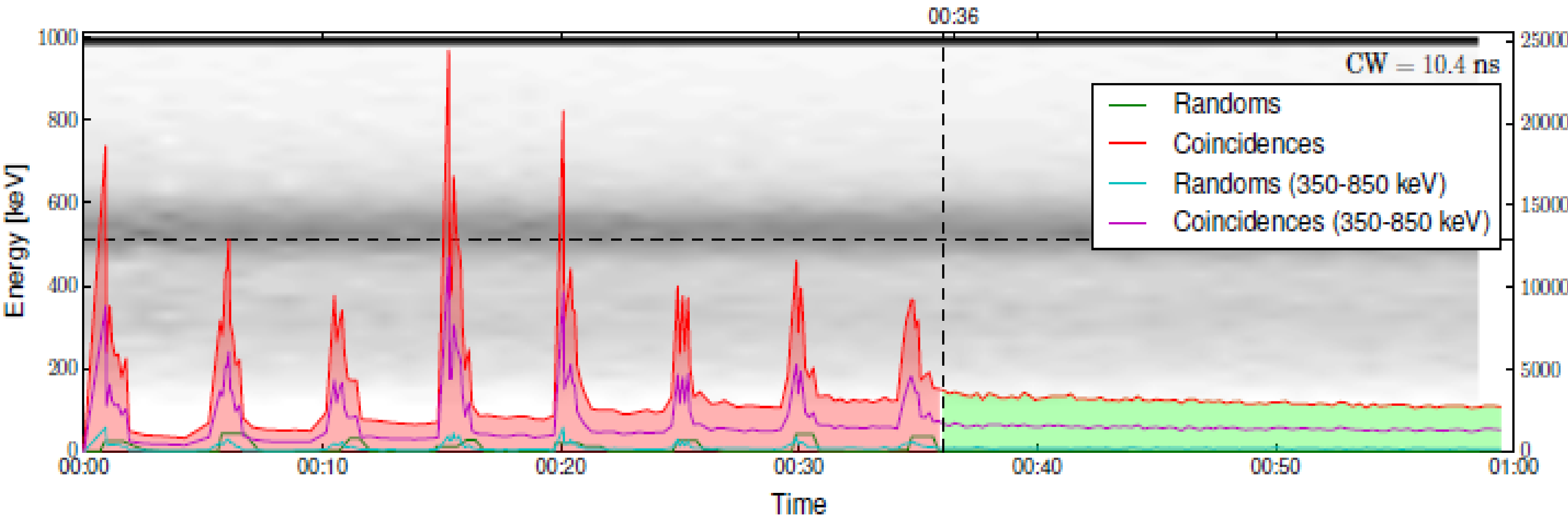

00:36
CW = 10.4 ns
Randoms
Coincidences
Randoms (350-850 keV)
Coincidences (350-850 keV)
Energy [keV]
Time
1000
800
600
400
200
0
25000
20000
15000
10000
5000
0
00:00
00:10
00:20
00:30
00:40
00:50
01:00

TPS → Dose-fraction irradiation → Complete treatment

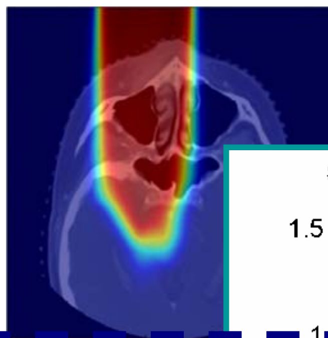

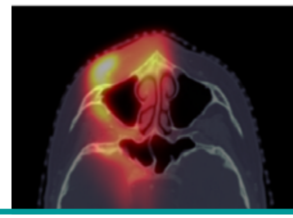

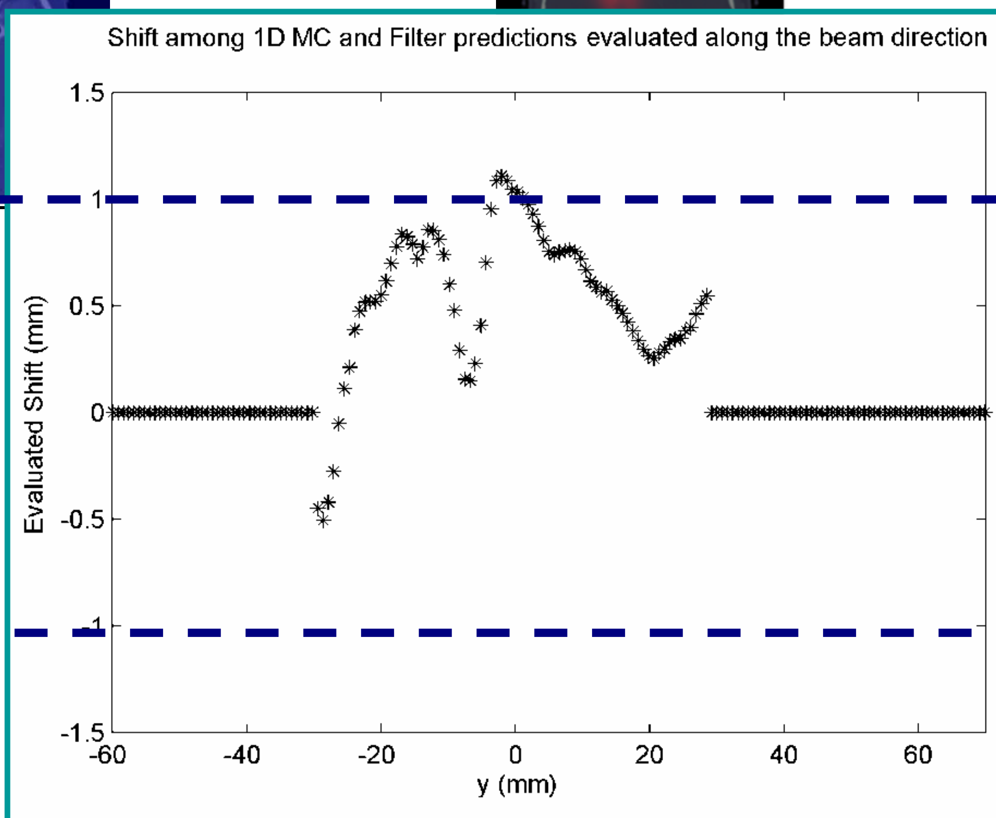

Differences between simulated and measured activity profiles

$\Delta = \pm 1mm$

PROGRAMMI DI RICERCA SCIENTIFICA DI RILEVANTE INTERESSE NAZIONALE
Anno 2010-2011 - prot. 2010P98A75

INSIDE aims to build a dedicated in-beam PET scanner, capable of:

- handling the count rate during the treatment
- reconstruct the Bragg peak position to 1 mm

» in less than 5 minutes since the beginning of dose delivery.

Keywords:

HADRON THERAPY
IN-BEAM PET
SILICON PHOTOMULTIPLIER (SiPM)

Monitoring: an open problem

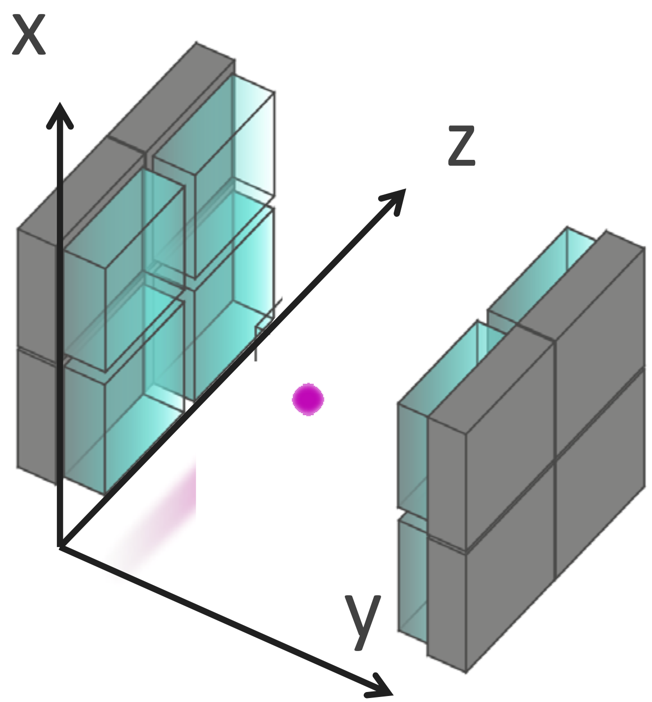

Performances of the PET prototype: a ^{22}Na point source at the center of the FOV

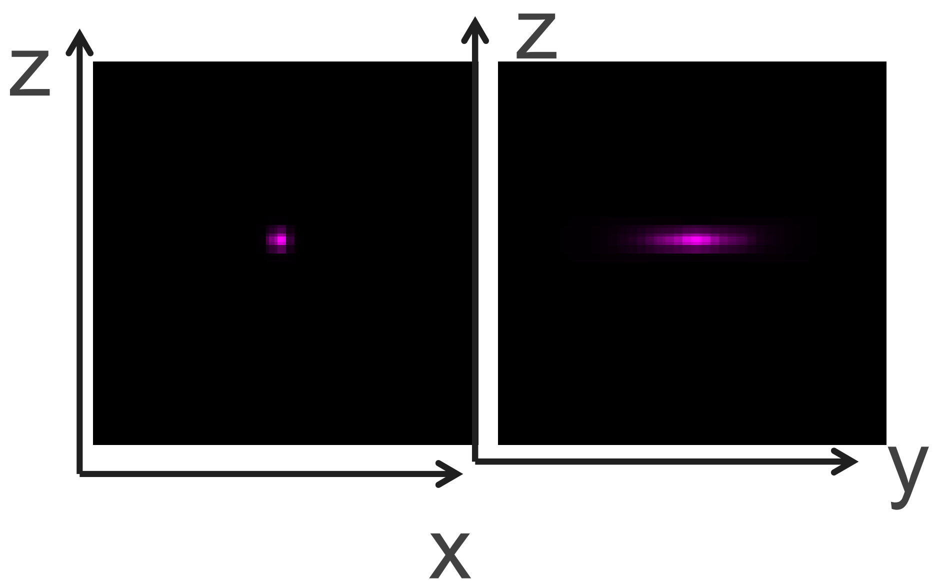

Central reconstructed slice in the xz (left) and yz (right) planes.

- Energy Resolution (FWHM)
  Head #1: 15.6%
  Head #2: 15.2%

- Spatial Resolution
  $FWHM_x$= 13 mm
  $FWHM_y$= 1.7 mm
  $FWHM_z$= 1.7 mm

SiPM!

Different geometry, size, microcell size and GF.

$40 \times 40 \mu m^2$ => GF 44%
$50 \times 50 \mu m^2$ => GF 50%
$100 \times 100 \mu m^2$ =

G.Bisogni, A. Del Guerra, B. Liu, N. Marino, M. Morrocchi

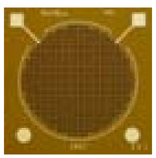

1mm ϕ

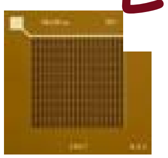

$1 \times 1 mm^2$

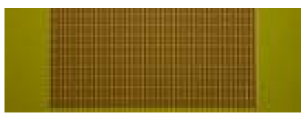

$2 \times 2 mm^2$

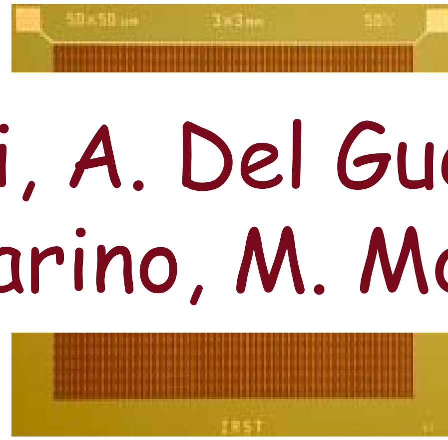

$3 \times 3 mm^2$ (3600 cells)

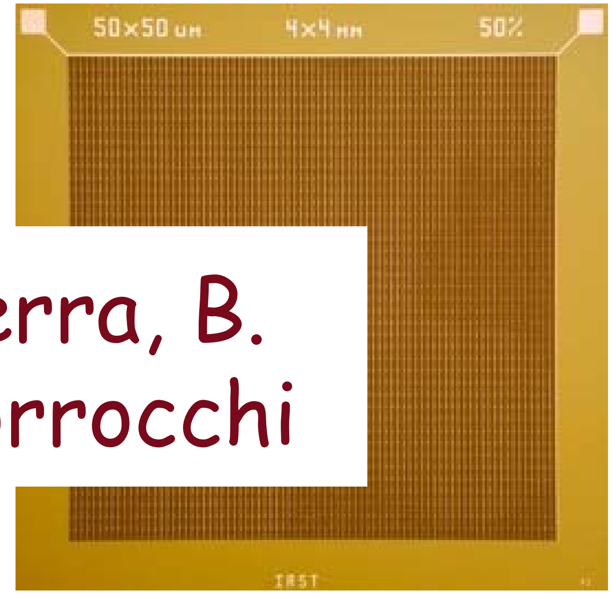

$4 \times 4 mm^2$ (6400 cells)

4 mm

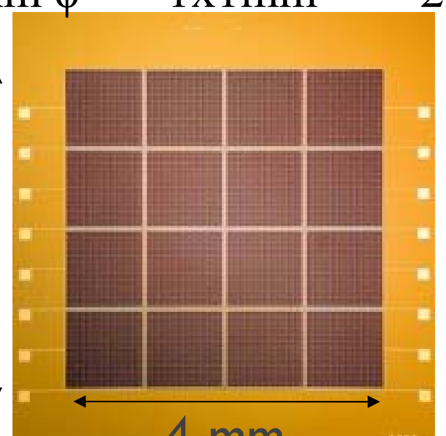

4 mm

$1.5 \times 1.5 mm^2$
8x8

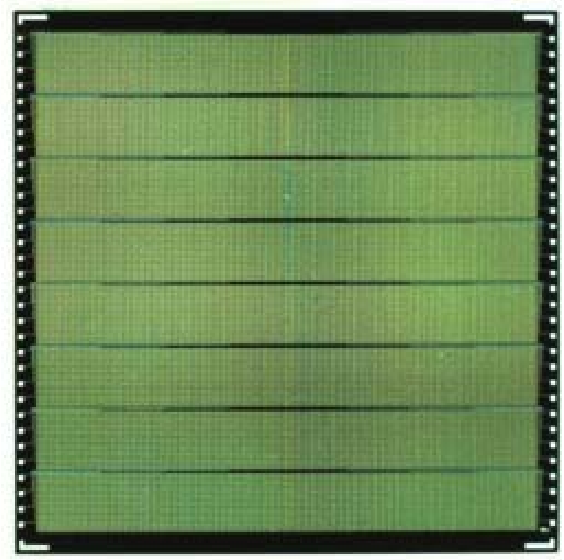

1.3cm

Sezioni di:
Bari, Bologna,
Pisa, Perugia,
Trento

SiPM: Energy resolution

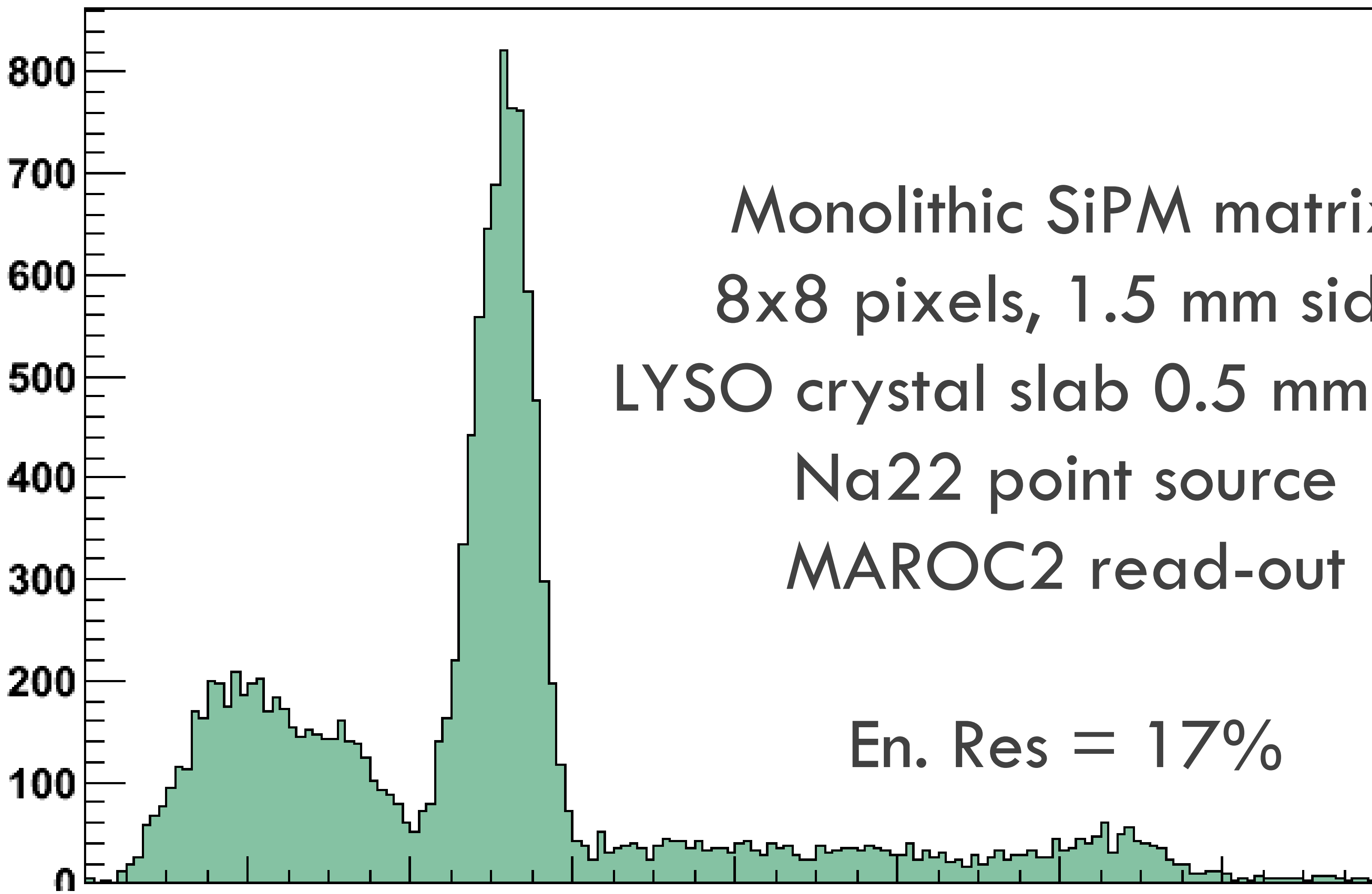

Monolithic SiPM matrix
8x8 pixels, 1.5 mm side
LYSO crystal slab 0.5 mm thick
Na22 point source
MAROC2 read-out

En. Res = 17%

SiPM: Time resolution

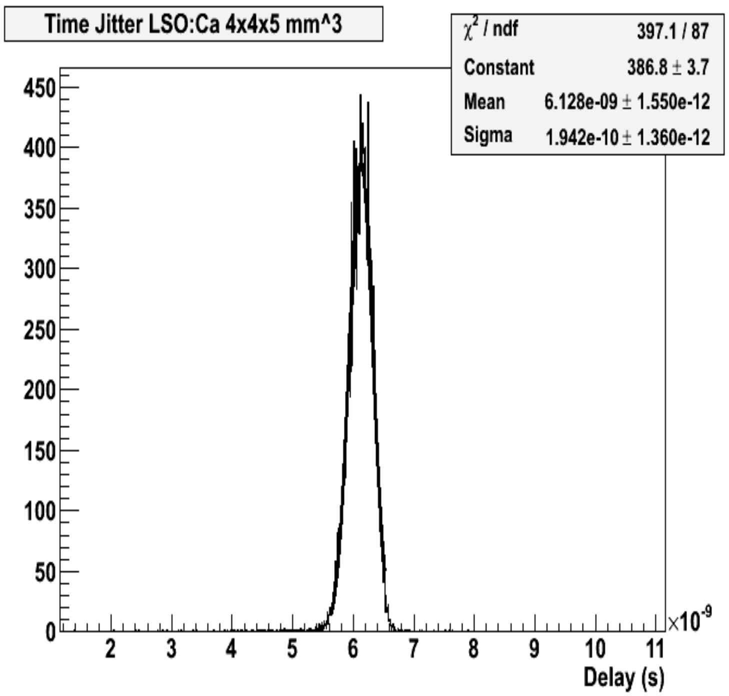

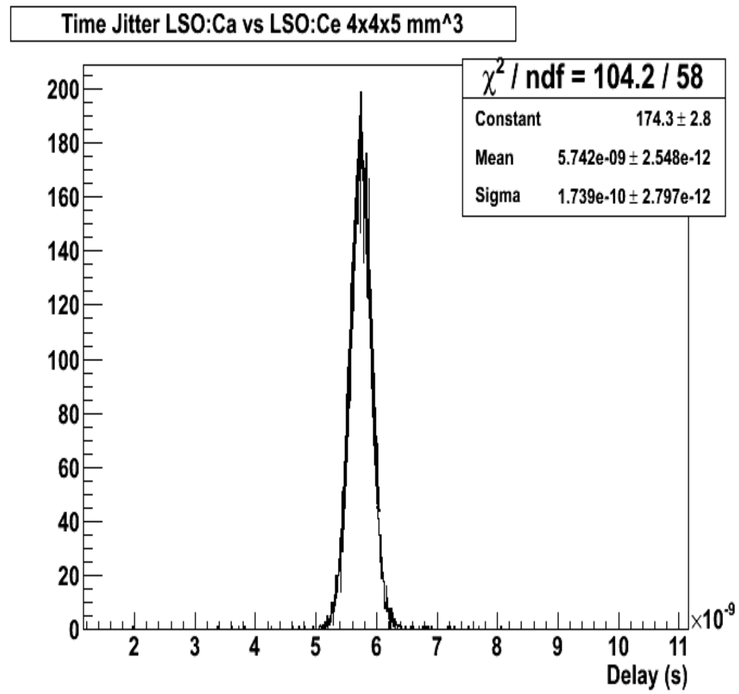

Table 2: Time resolution at $511 keV$ of the tested samples

LSO Ca %	Size (mm^3)	FWHM (ps)	$\sigma\sqrt(2)$ (ps)
0	$2 \times 2 \times 10$	345	104
0.3	$3 \times 3 \times 10$	357	107
0	$4 \times 4 \times 5$	475	143
0.3	$4 \times 4 \times 5$	427	128

SiPM: Spatial Resolution

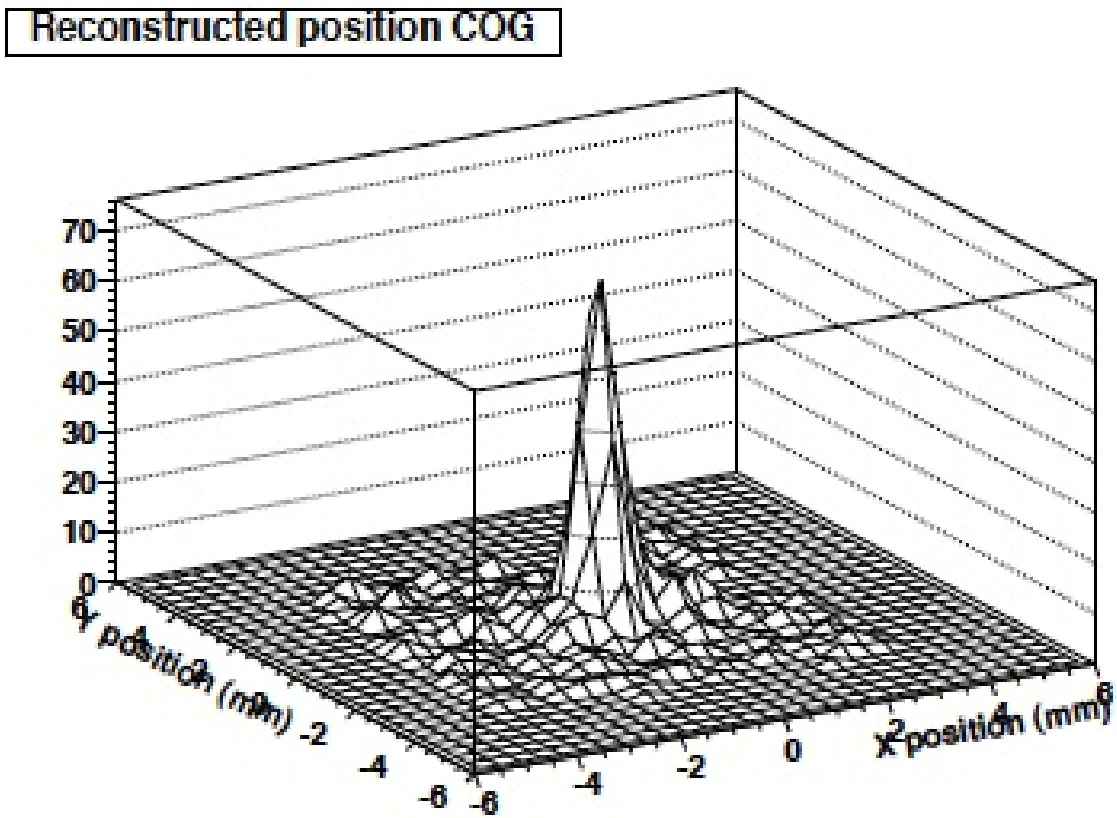

Reconstructed position with center of gravity algorithm. The spatial resolution is about **1 mm FWHM** as obtained with a standard center of gravity algorithm.

TOF system

✓TOF-PET systems exploit the time difference between the two emitted photons to better locate the annihilation position.

✓The limit in the annihilation point location is mainly due to the error in the time difference measurement , namely the time resolution **Δt** of the coincidence system

✓ Time resolution is used by the reconstruction algorithm to locate the annihilation point **Δx** (**Δx** =c Δt/2)

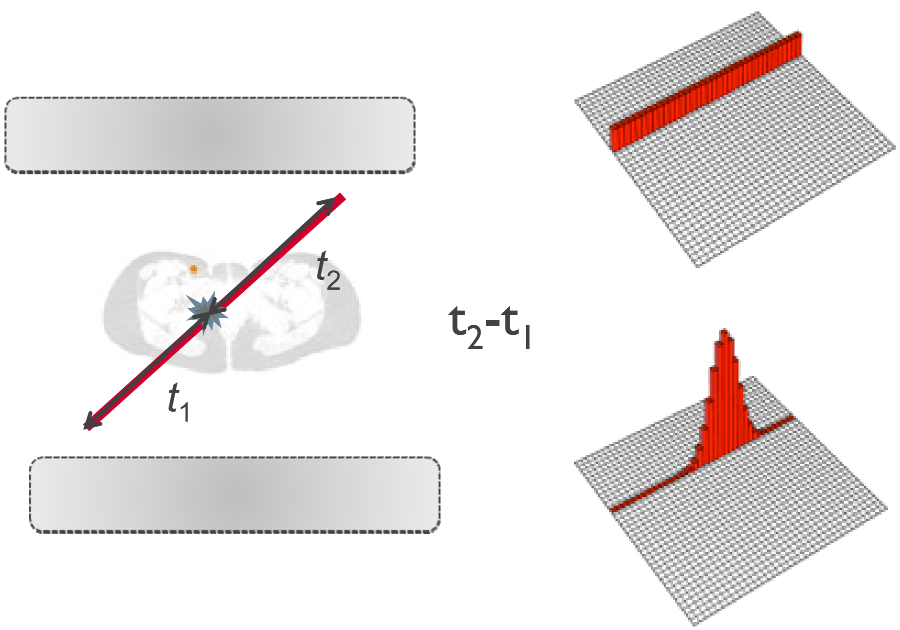

PET traditional

The probability for the event to be located along the LOR is uniform

PET Time-of-Flight

The most likelihood position is in the center of the error distribution

4DMPET Detector module

A continuous fast scintillating crystal coupled on both sides to arrays of SiPM

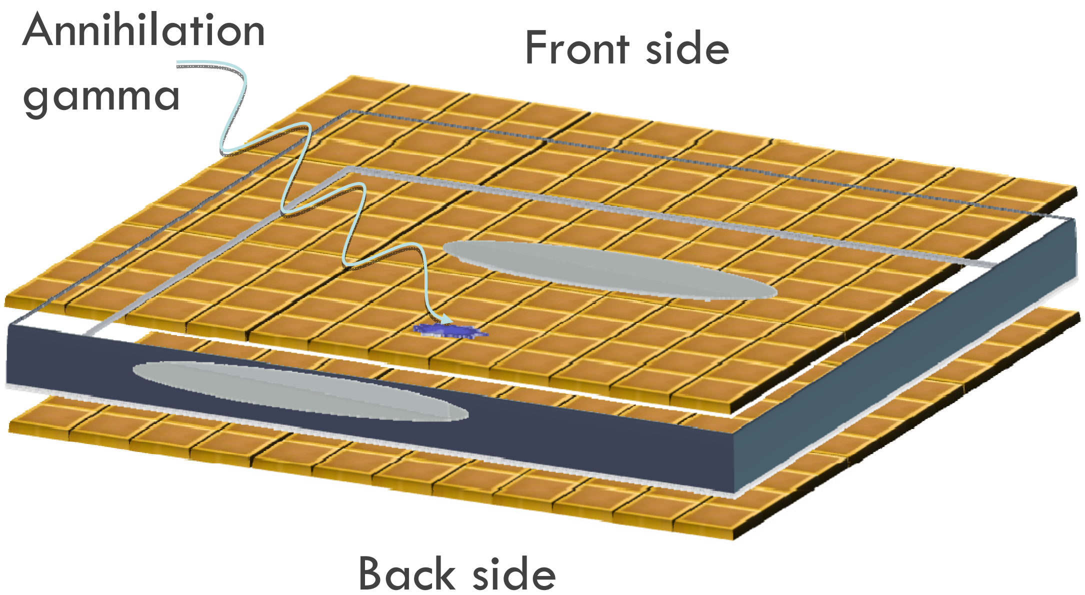

For every event, the timing and the energy released in the crystal at the pixel level will be acquired

Depth Of Interaction (DOI) information to improve the spatial resolution of the detector to the ultimate goal of 0.5 mm FWHM in X-Y and of 2 mm FWHM in DOI.

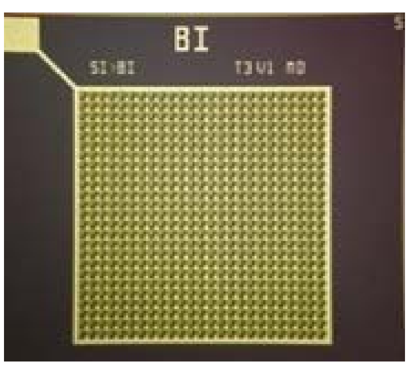

INFN
Istituto Nazionale di Fisica Nucleare

MRI compatible

Bari, Pisa, Perugia, Torino

The <u>first ever</u> Italian 7T whole-body MR system for human application is operative at the IMAGO7 Foundation (Pisa).

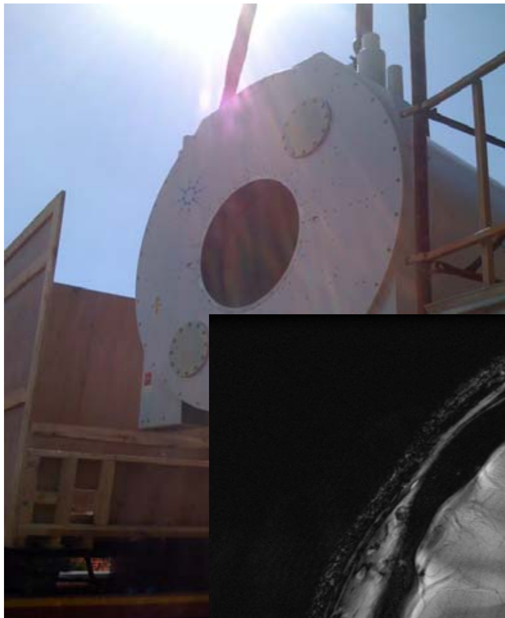

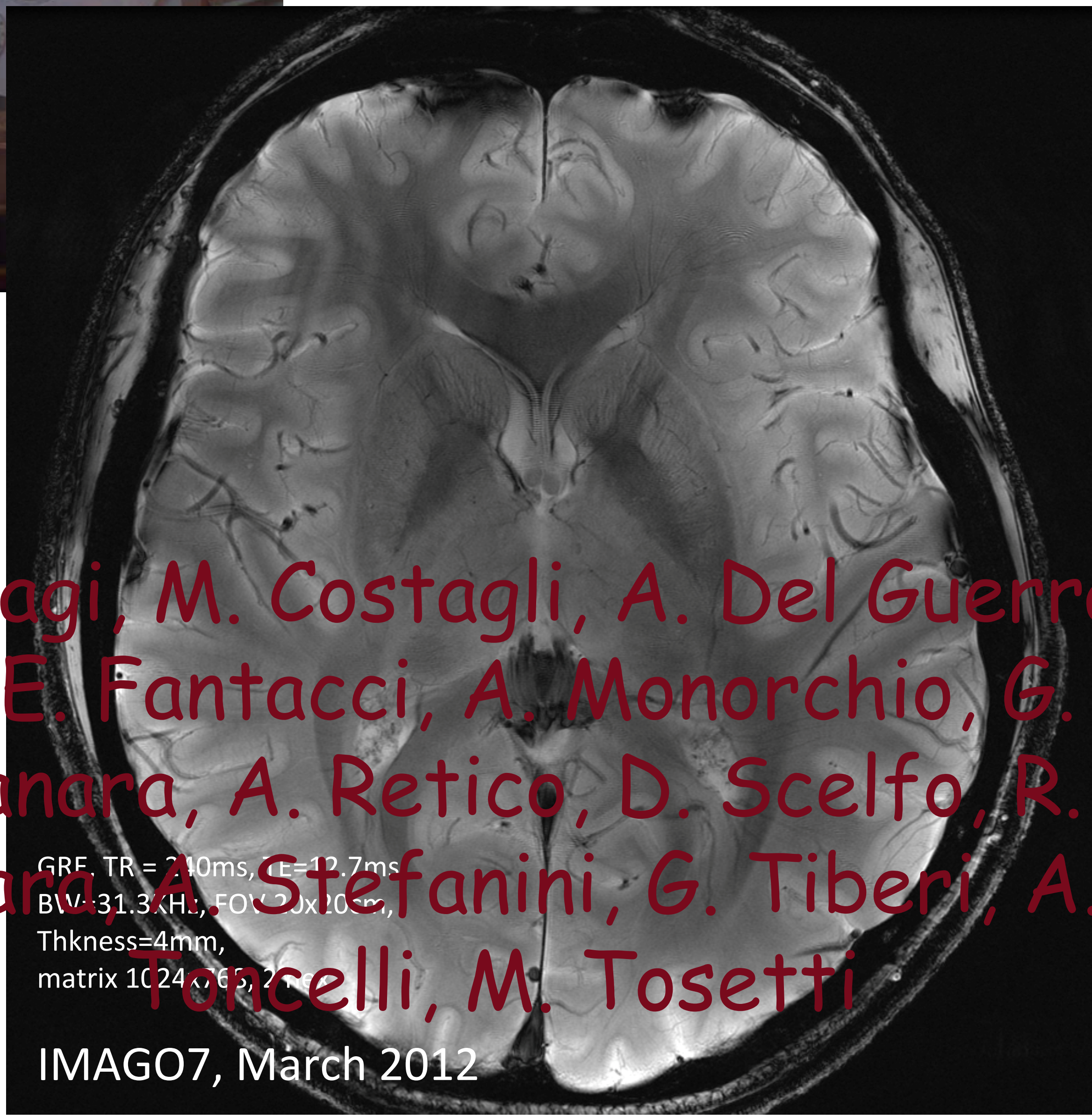

L. Biagi, M. Costagli, A. Del Guerra, M.E. Fantacci, A. Monorchio, G. Manara, A. Retico, D. Scelfo, R. Stara, A. Stefanini, G. Tiberi, A. Toncelli, M. Tosetti

IMAGO7

FONDAZIONE STELLA MARIS
ISTITUTO DI RICOVERO E CURA A CARATTERE SCIENTIFICO

UNIVERSITÀ DI PISA

Azienda Ospedaliero Universitaria Pisana

"Eugenio Medea"
Istituto di Ricovero e Cura a Carattere Scientifico

la Fondazione CariPisa

INFN

Scuola Superiore Sant'Anna Pisa

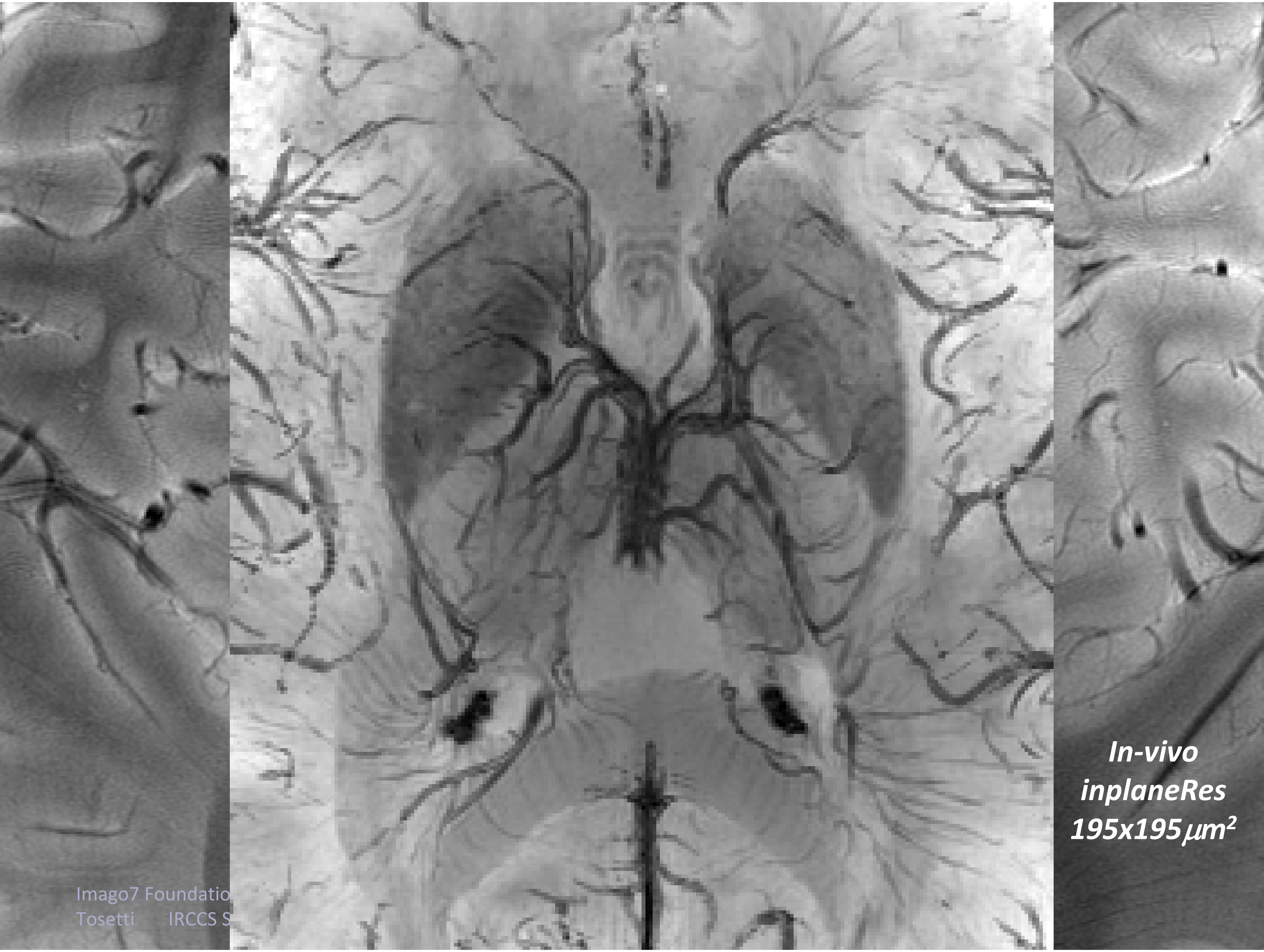
In-vivo
inplaneRes
195x195μm^2
Imago7 Foundatio
Tosetti IRCCS S

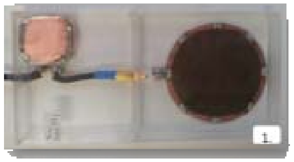

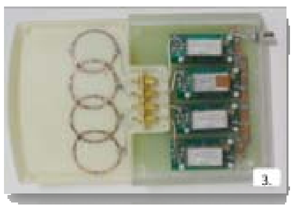

Radiofrequency coil development for Ultra-High Field magnetic resonance

INFN
Istituto Nazionale di Fisica Nucleare

PI & AQ - Dual-tuned (DT) surface RF coils (^{1}H and ^{31}P) :

•simulation of many different coil designs to reach the channel decoupling;

•final 7 T design integrated to the 7 T scanner in Pisa.

DT coil @ 7 T on flat holder

DT coil @ 7 T on curve holder

A. Retico - TESLA

B and E field simulations

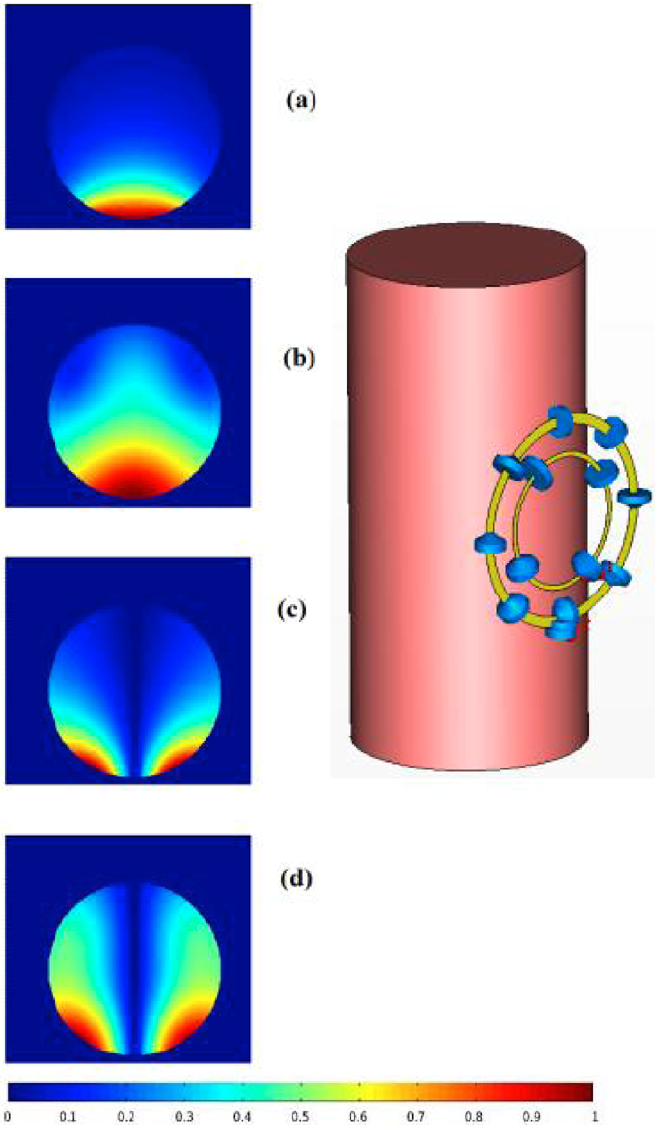

- B_1 field simulated at 120.6 MHz (a) and at 298 MHz (b) on a transverse plane of the phantom;
- E field simulated at 120.6 MHz (c) and at 298 MHz (d) on a transverse plane of the phantom.

In magnet tests

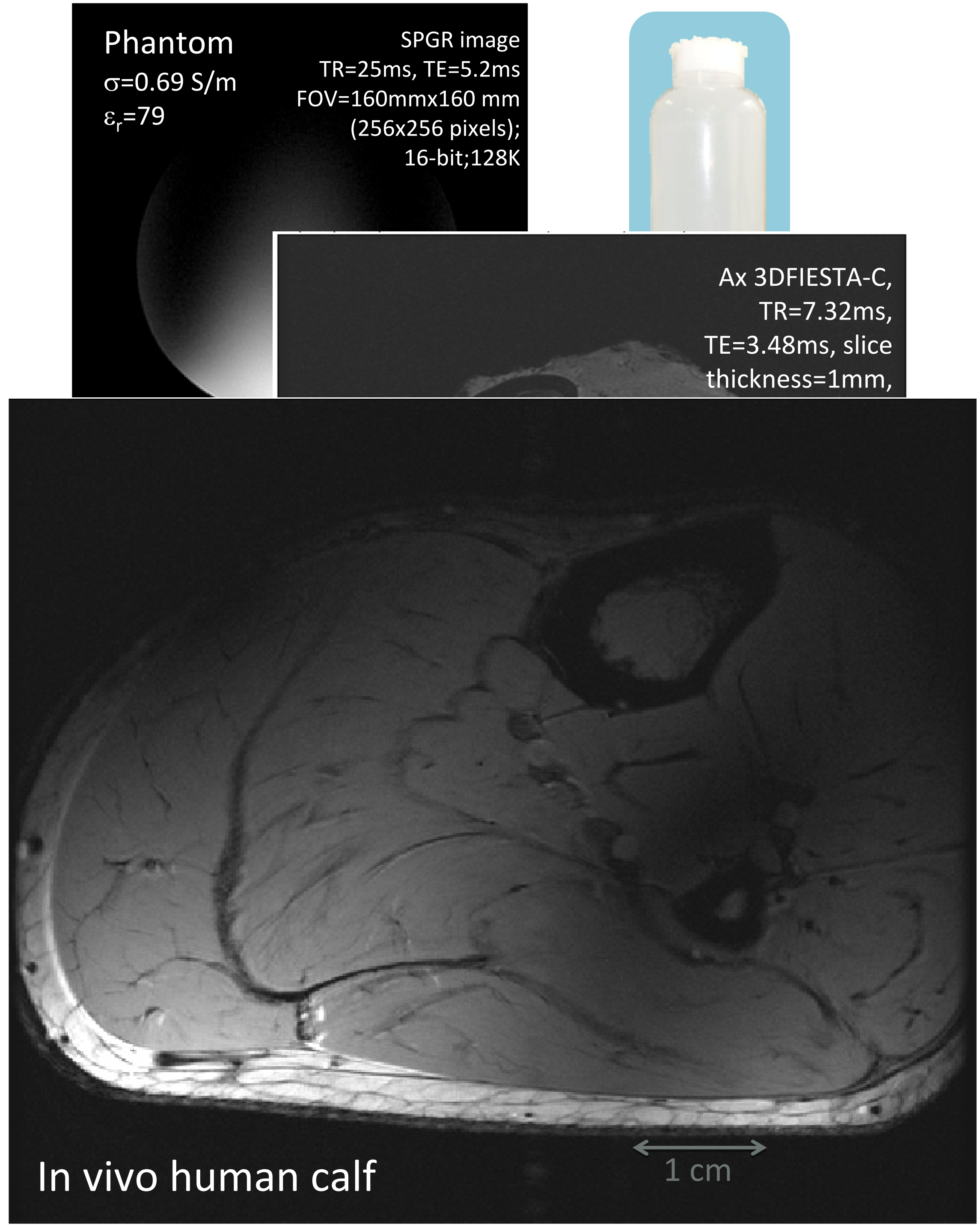

TESLA

7T MR

WP1.

NEW COILS:

•32 ch. Rx - Phased Array for human knee imaging

•Tx-Rx surface coil fo human neck

•Tx-Rx volume coil for small animals

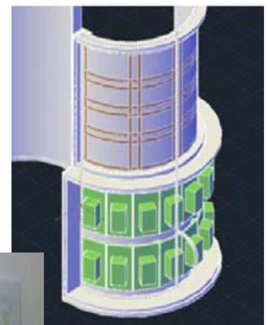

SAFETY:

•Electromagnetic Simulations

- Power deposition in biological tissues (SAR): computation of SAR maps for real-time monitoring at 7T

1.5T, 3T, 7T MR

WP2.

IMAGE PROCESSING and ANALYSIS:

•Postprocessing of 7T image to attenuate inhomogeneities.

•Image segmentation (cartilages, tendons and bones) and quantitative image parameter computation.

•Evaluation of the predictive value of MRI data on clinical data (1.5T and 3T) and feasibility study on 7T data:

- Structural MRI (neurodegenerative diseases);
- Diffusion weighted imaging (brain tumor segmentation and characterization, connectivity map interpretation, …)

Image Processing and Analysis of 7T data

- Postprocessing of 7T brain images to attenuate inhomogeneities.

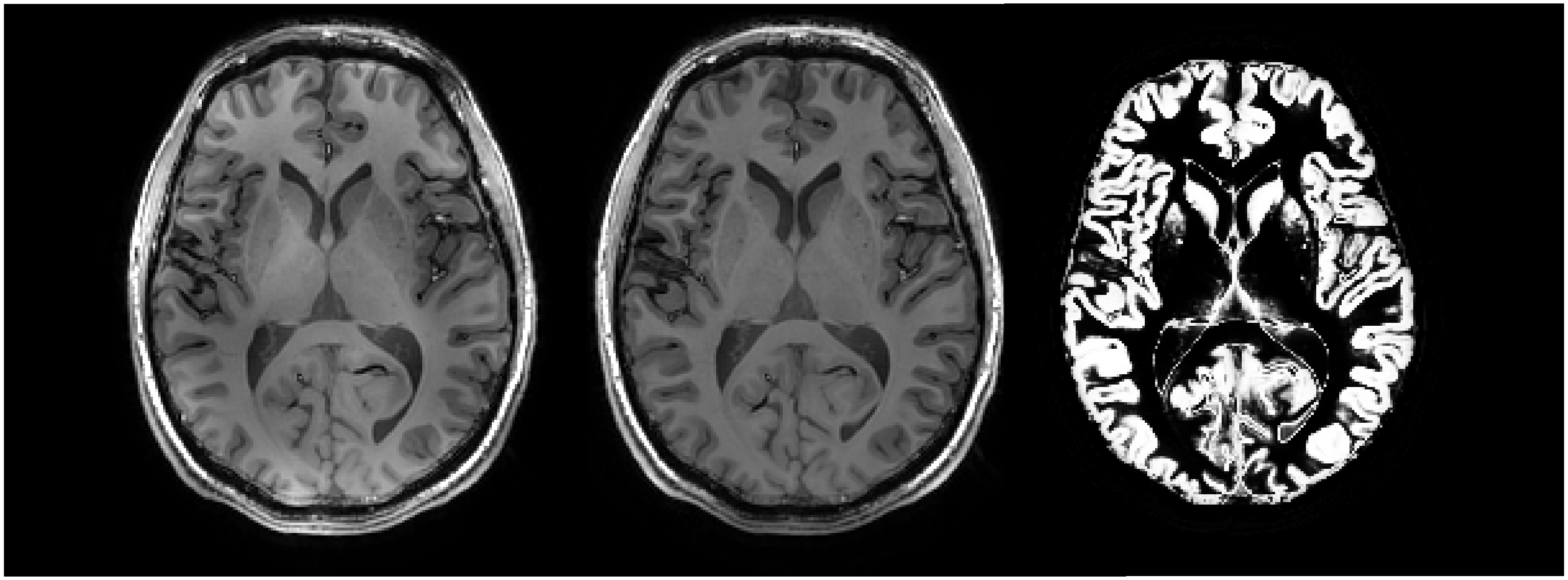

- Quantification of bone architecture to assessment fracture risk and to measure the efficacy of therapeutic interventions in bone disease.

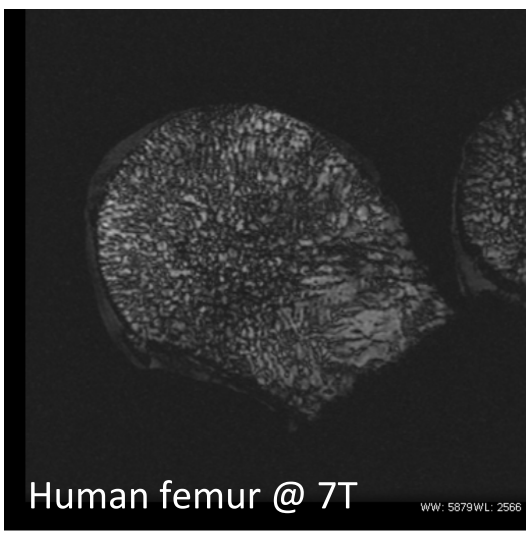

Image segmentation (cartilages, tendons and bones) and quantitative image parameter computation: total bone volume (TBV), bone volume fraction (BVF), surface curve ratio (SCR), erosion index (EI)

Magnetic susceptibility effects

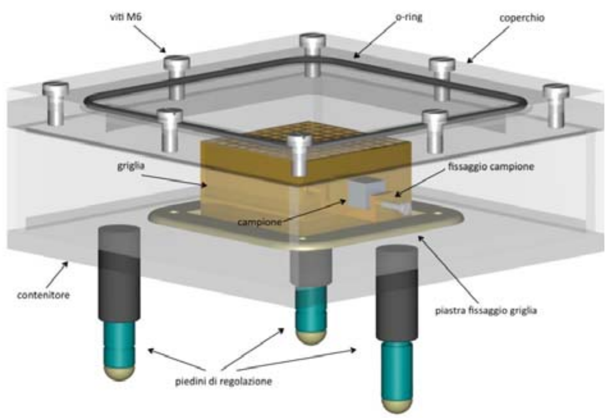

MR-CompatibilePhantom
χ insert

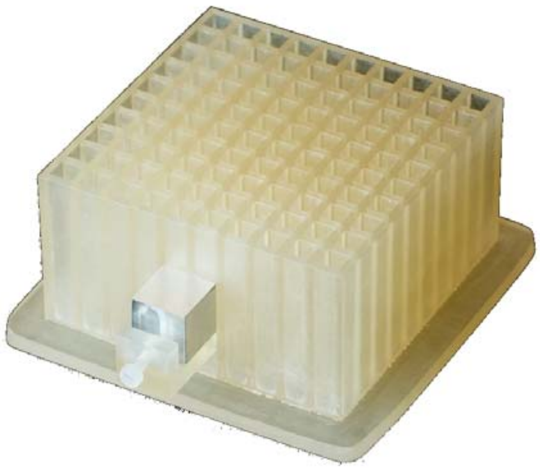

+ Titanium
Susceptibility = 1.807x10^-4
7T–distorsion: 33.3mm

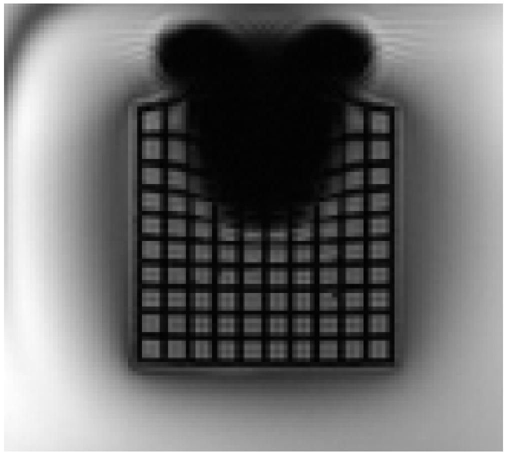

+ Ergal
Susceptibility = 2.11x10^-5
7T–distorsion: 13.52mm

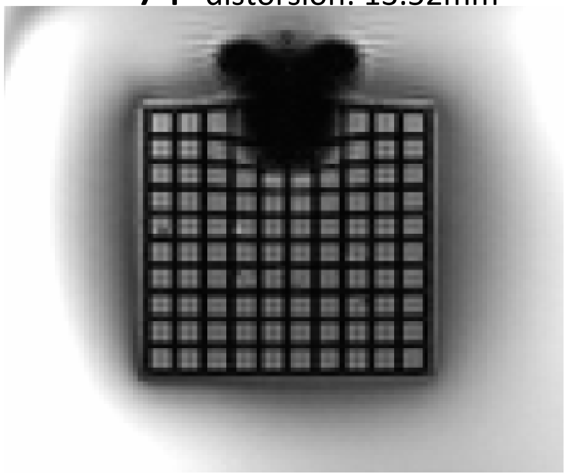

Potenziali applicazioni nel campo dell'imaging pre-clinico: dalla PET/CT alla PET/MR

Small animal PET/SPECT system YAP-(S)PET.
Tecnologia: Scintillatori (YAP:Ce) e PS-PMT

Small animal CT system XaltHR*.
Tecnologia: CMOS detectors e microfocus X-ray source

*in collaboration with IFC-CNR Pisa

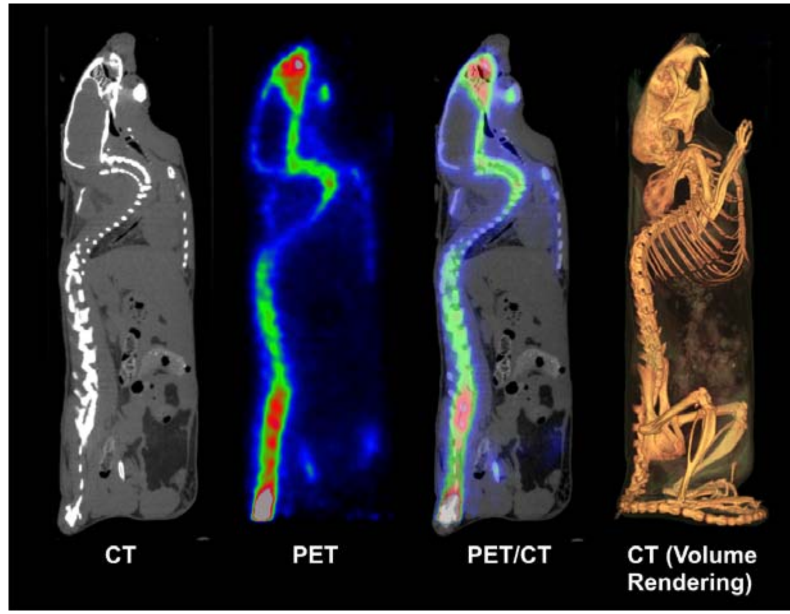

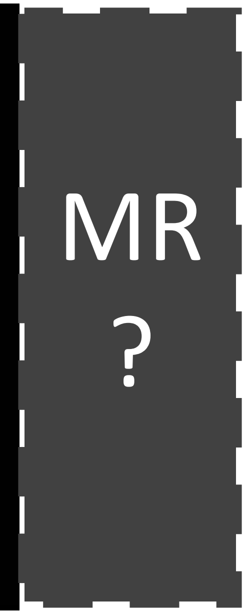

Applicazioni di imaging multimodale su topo: PET con ^{18}F combinato con una CT.
Da sinistra: immagine CT, immagine PET e fusione delle immagini.

Utilizzando un modulo di rivelazione PET basato su fotorivelatori compatibili con il campo magnetico come i SiPM è possibile sviluppare sistemi PET/MR "fully integrated" capaci di imaging PET e MR simultaneo.

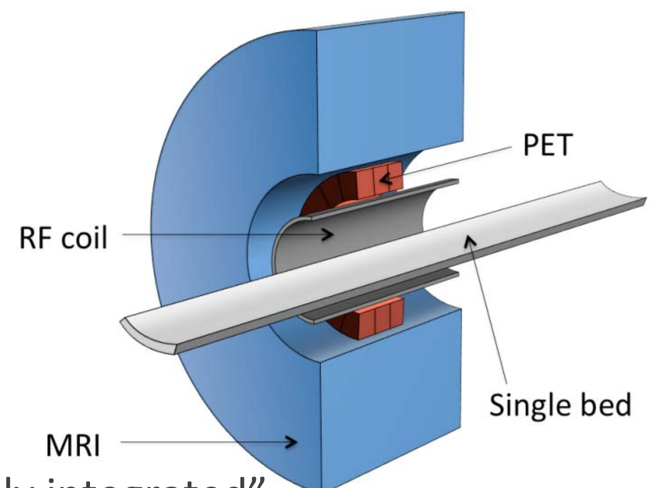

A destra: possibile configurazione di un sistema PET/MR "fully integrated"

X-RAY PHASE CONTRAST IMAGING

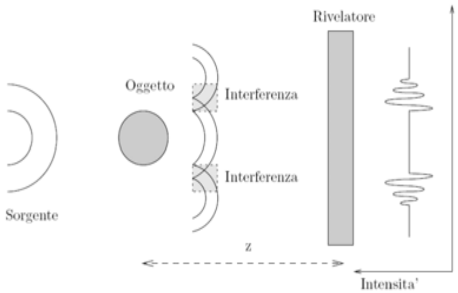

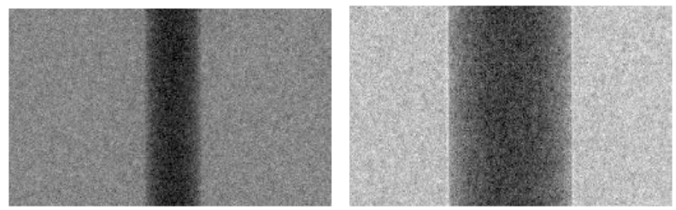

(a) Immagine in assorbimento

(b) Edge - enhancement

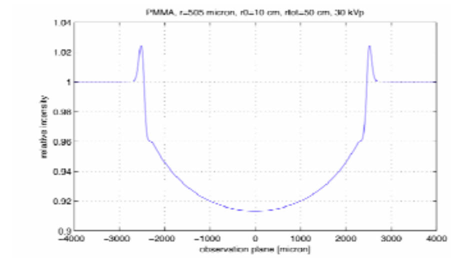

Simulazione

Tecnica in-line ed edge enhancement

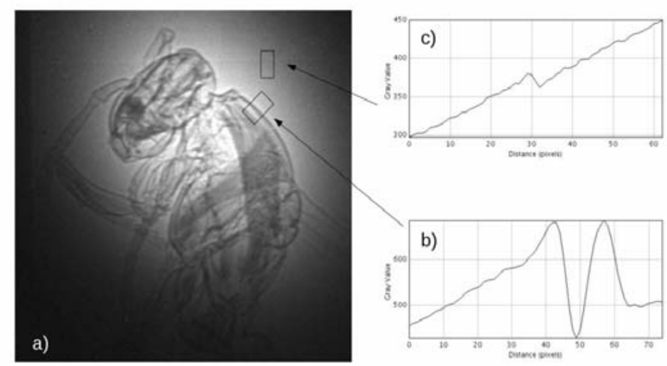

Analisi quantitativa delle immagini con contrasto di fase

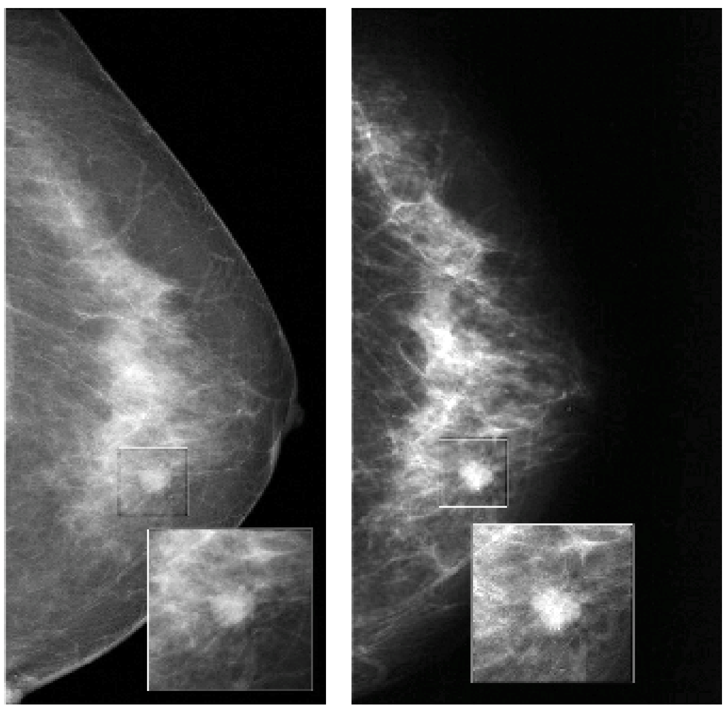

Applicazioni cliniche dimostrate

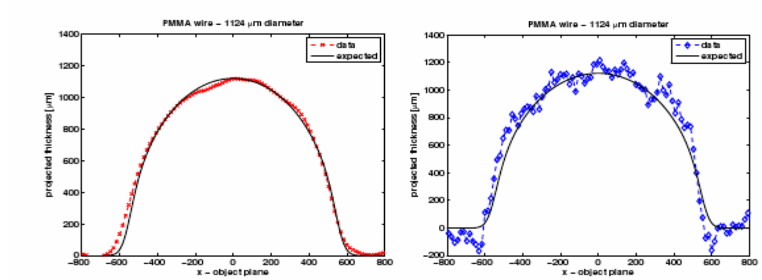

Phase retrieval